

## **General Disclaimer**

### **One or more of the Following Statements may affect this Document**

- This document has been reproduced from the best copy furnished by the organizational source. It is being released in the interest of making available as much information as possible.
- This document may contain data, which exceeds the sheet parameters. It was furnished in this condition by the organizational source and is the best copy available.
- This document may contain tone-on-tone or color graphs, charts and/or pictures, which have been reproduced in black and white.
- This document is paginated as submitted by the original source.
- Portions of this document are not fully legible due to the historical nature of some of the material. However, it is the best reproduction available from the original submission.

**A THEORETICAL STUDY OF HETEROJUNCTION  
AND GRADED BAND GAP TYPE SOLAR CELLS**

Final Report on  
NASA Grant No.  
NSG 1116

**(NASA-CR-158232) A THEORETICAL STUDY OF  
HETEROJUNCTION AND GRADED BAND GAP TYPE  
SOLAR CELLS Final Report (North Carolina  
State Univ.) 51 p HC A04/MF A01 CSCL 10A**

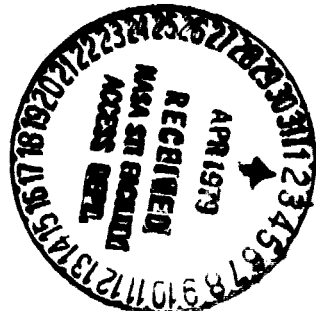
**N79-19452**

**Unclas  
G3/44 16401**

March 1979

J.P.C. Chiang and J. R. Hauser

North Carolina State University  
Electrical Engineering Department  
Raleigh, NC 27650



#### ABSTRACT

This report summarizes work performed on NASA Grant No. NSG 1116 during the period of January 1, 1977 through December 31, 1978. The work during this period has concentrated on including multi-sun effects, high temperature effects, and electron irradiation effects into the computer analysis program for heterojunction and graded bandgap solar cells. These objectives have been accomplished and the program is now available for such calculations.

This report is written in the form of three manuscripts which have been prepared for publication. Details of the device modeling and computer analysis techniques used to study solar cells have been contained in earlier annual reports on this grant and are not repeated here.

EFFECTS OF TEMPERATURE AND INTENSITY  
ON THE OPTIMUM BANDGAP OF AlGaAs SOLAR CELLS\*

J. P. C. Chiang and J. R. Hauser  
North Carolina State University  
Raleigh, NC 27650

ABSTRACT

The optimum bandgap for single junction solar cells operated at AM0, 1 sun conditions and at 300°K is known to occur at a value close to that of GaAs. This work shows that with increasing temperature and/or increasing optical intensity the optimum bandgap moves to larger values. Detailed computer calculations for AlGaAs cells are presented which illustrate the optimum bandgaps in this material at various temperatures and solar intensities.

---

\*This work was supported by a NASA Langley research grant.

## 1. INTRODUCTION

The optimum energy bandgap of single junction solar cells has been investigated in several previous papers [1-3]. Early studies of solar cells based upon simple device models have predicted that the optimum energy bandgap is around 1.4-1.6 eV for AMO, 1 sun, room temperature operation. More recent detailed numerical calculations on specific semiconductors of GaInAs and AlGaAs have shown that the AlGaAs/GaAs heterojunction cell with an active cell bandgap of about 1.44 eV is very close to the optimum bandgap [4].

The present work discusses detailed calculations of heterojunction solar cell performance at increasing temperature and illumination levels. In order to make the analysis as realistic as possible, the specific ternary III-V alloys  $\text{Ga}_{1-x}\text{In}_x\text{As}$  and  $\text{Al}_{1-x}\text{Ga}_x\text{As}$  have been selected to be studied. The  $\text{Ga}_{1-x}\text{In}_x\text{As}$  provides a semiconductor with bandgaps below that of GaAs and  $\text{Al}_{1-x}\text{Ga}_x\text{As}$  provides values above that of GaAs. From these studies the optimum bandgap for heterojunction type solar cells at elevated temperature and light intensity can be identified using a practical set of material parameters.

## 2. DEVICE MODELING

The calculations of this work were made using a detailed numerical simulation of heterojunction solar cells. Details of the device modeling and numerical techniques have been previously discussed [5,6]. The computer analysis program solves the basic device differential equations appropriate to heterojunction or graded bandgap solar cells providing data on the terminal properties of solar cells such as open circuit voltage,

short circuit current, fill factor and maximum efficiency. Input to the program is a detailed set of material and device parameters from which the material properties of any desired  $\text{Al}_{1-x}\text{Ga}_x\text{As}$  or  $\text{Ga}_{1-x}\text{In}_x\text{As}$  alloy can be determined.

The additional modeling which is pertinent to the present work is the manner in which temperature effects are incorporated into the model. For operation around room temperature, both the direct and indirect bandgaps of the binary semiconductors AlAs, GaAs and InAs were assumed to be decreased linearly with temperature as

$$\epsilon_g = \epsilon_{g0} - \alpha(T - T_0), \quad (1)$$

where  $\epsilon_{g0}$  is the bandgap at  $T = T_0$  (300°K). Table I gives a list of the temperature coefficients used in the analysis. For the ternary alloys,  $\alpha$  was assumed to vary linearly with composition.

The temperature dependence of mobility was taken to be of the form

$$\mu = \mu_0 (T/T_0)^m, \quad (2)$$

where  $\mu_0$  is the mobility at temperature  $T_0$  (300°K) and  $m$  is an experimentally measured constant. For holes and direct bandgap electrons the temperature dependence was assumed to be that of GaAs with  $m = -2.3$  for electrons [7,9] and  $m = -2.0$  for holes [9]. For the indirect bandgap electrons  $m = -2.3$ , which has been reported for AlAs, was used [7]. While these temperature dependences may not be exact for all alloy compositions, optimum solar cells have bandgaps close to that of GaAs and thus this approach should give a good approximation. Also the indirect bandgap is only important

Table I. Bandgap temperature coefficients

Material	$\alpha$ (eV/°K)	
	Direct Bandgap	Indirect Bandgap
InAs	$3.5 \times 10^{-4}$ [7]	$4.0 \times 10^{-4}$ [7]
GaAs	$4.3 \times 10^{-4}$ [8,9]	$4.0 \times 10^{-4}$ [7]
AlAs	$4.3 \times 10^{-4}$ [10]	$4.0 \times 10^{-4}$ [7]

for  $\text{Al}_{1-x}\text{Ga}_x\text{As}$  compositions near AlAs and this is the justification for using the AlAs data for the indirect bandgap.

For the purpose of this work, minority carrier lifetime was assumed to be independent of temperature. There is no intrinsic reason to assume this is true, however insufficient data is available on solar cell quality III-V material to more accurately model lifetime at this time.

The specific solar cell device structure which has been studied is shown in Figure 1. It consists of a p-type base layer of approximately 125  $\mu\text{m}$  in thickness. A wide bandgap  $\text{Al}_{1-x}\text{Ga}_x\text{As}$  window layer is present at the top of the cell. The p-n junction is taken to be at some small distance below the heterojunction. Finally an SiO antireflecting layer is present on the front surface of the cell.

From previous studies of such cells with a GaAs base layer and an  $\text{Al}_{1-x}\text{Ga}_x\text{As}$  window layer, it has been found that the optimum antireflecting layer thickness is about .07  $\mu\text{m}$ , and the optimum p-n junction depth is about 0.3  $\mu\text{m}$  below the window layer [5,6]. These values were used in the present study along with a window layer thickness of 0.1  $\mu\text{m}$ . While the

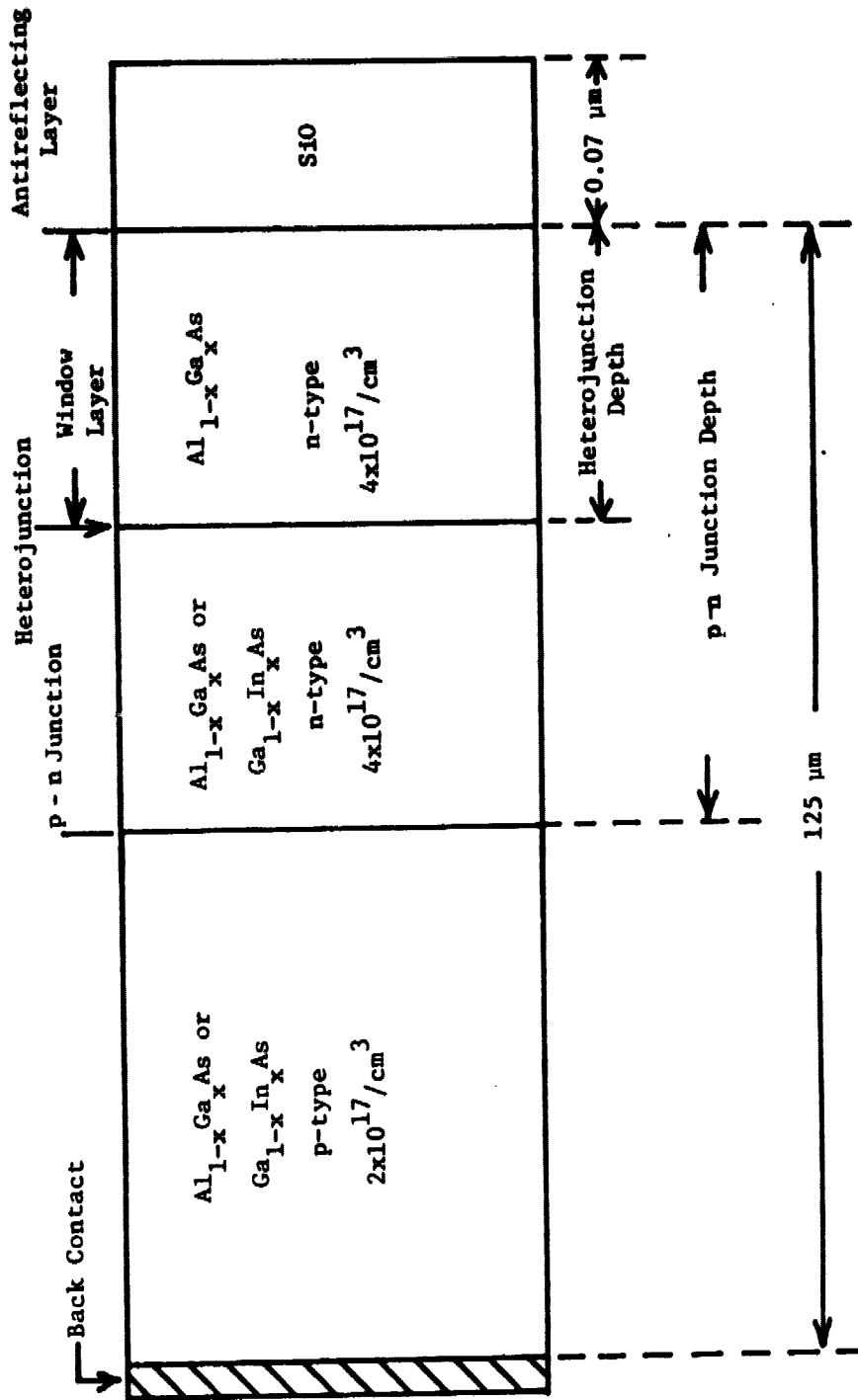


Figure 1. Heterojunction Solar Cell Device Structure.



optimum window layer thickness is less than 0.1  $\mu\text{m}$  this value was selected as a realistic practical value. While the selected junction depths may not be optimum values for all alloy compositions, temperatures and/or light intensities, it was decided to keep these fixed in order to study only the effects of temperature and solar intensity on the optimum bandgap.

The composition of the window layer was fixed during this present study at 100% AlAs. This is somewhat larger than the value used in most present day AlGaAs/GaAs cells. This represents the ideal upper limit on the bandgap of the window layer using AlGaAs. However compositions of 90% AlAs have bandgaps which are only slightly less than the pure AlAs and do not degrade performance significantly.

### 3. EFFECTS OF TEMPERATURE ON PERFORMANCE

The first calculations to be discussed are for conventional type heterojunction cells with pure GaAs as the base layer semiconductor. These illustrate the effects of temperature on heterojunction cells and provide a base of comparison for cells with other alloy compositions.

Figure 2 shows the calculated dark J-V characteristics for a GaAs base layer cell at 300°K and 500°K. The dark current increases by over four orders of magnitude (note scale change) for 500°K operation. At either 300°K or 500°K the region of operation (near  $I_{sc}$ ) is within a current region where the device exhibits near ideal diode behavior. The  $m=1$  or 2 values in Figure 2 refer to the diode factor  $m$  in an equation of the form

$$J = J_0 \exp(qV/mkT). \quad (3)$$

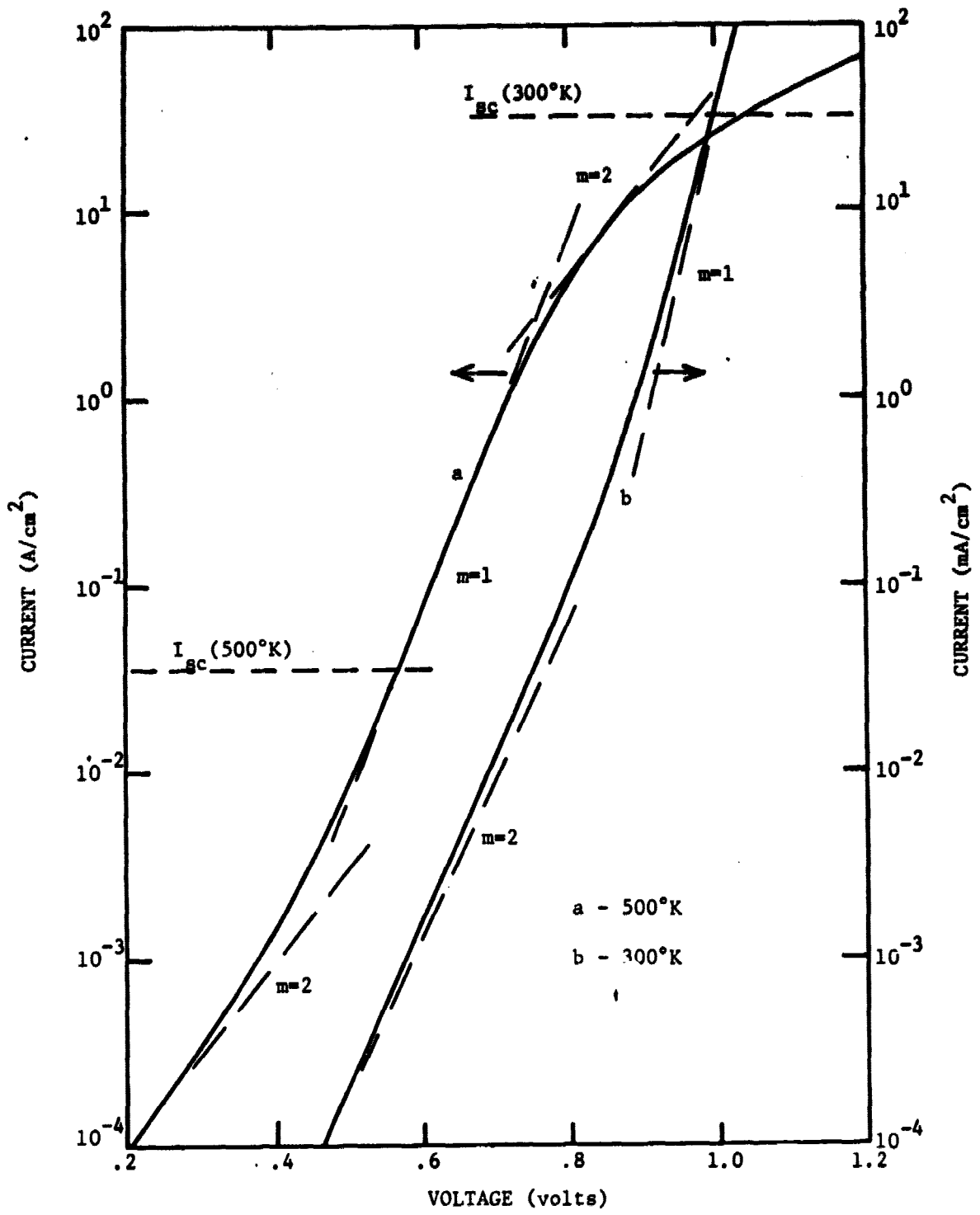


Figure 2. Dark I-V Characteristics for GaAs Base Layer Cell at Two Temperatures.

The 500°K curve shows a transition to the high injection region of operation at around 0.8 volt. This region becomes important when such a cell is operated at both high temperature and multi-sun illumination conditions as will be discussed in the next section.

The terminal J-V characteristics under 1 sun, AMO illumination for the GaAs cell are shown in Figure 3. As temperature increases, the open circuit voltage decreases, short circuit current increases, the fill factor decreases and efficiency decreases. All of these changes are expected except perhaps the increase in short circuit current which deserves some discussion. The increase in  $J_{sc}$  is due mainly to the decrease in bandgap of the semiconductor with increasing temperature. With the temperature dependence of mobility and diffusion coefficient used in the modeling, the diffusion length will decrease with temperature, since  $D \propto T^{m+1}$  and  $m \leq -2.0$ . However this decrease is not sufficient to offset the increase in absorption and  $J_{sc}$  increases.

Figure 4 show the variation of the major solar cell parameters with temperature for the GaAs base layer cells. The predicted decrease in  $V_{oc}$  is 2.16 mV/°K. The increasing short circuit current with increasing temperature partly offsets the decreasing fill factor and the resulting efficiency decreases only slightly faster than the open circuit voltage decreases.

In the next series of studies the terminal solar cell device parameters were investigated as a function of the composition of the base layer of the heterojunction cell. The window layer was kept fixed in composition but  $Ga_{1-x}In_xAs$  or  $Al_{1-x}Ga_xAs$  was substituted in the model for the material in which the p-n junction is located. The results of this

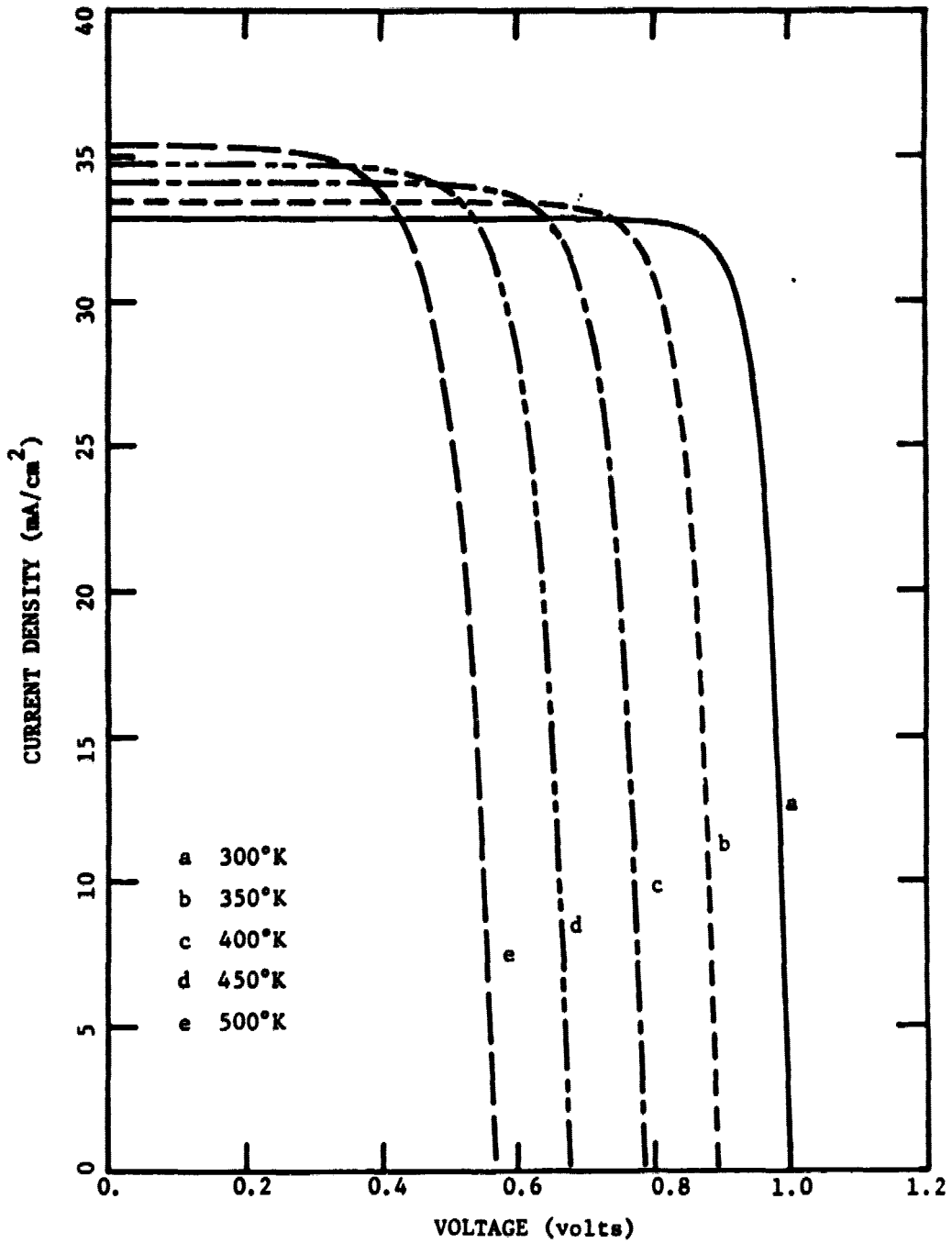


Figure 3. Effects of Temperature on Light J-V Characteristics for GaAs Base Layer Cell.

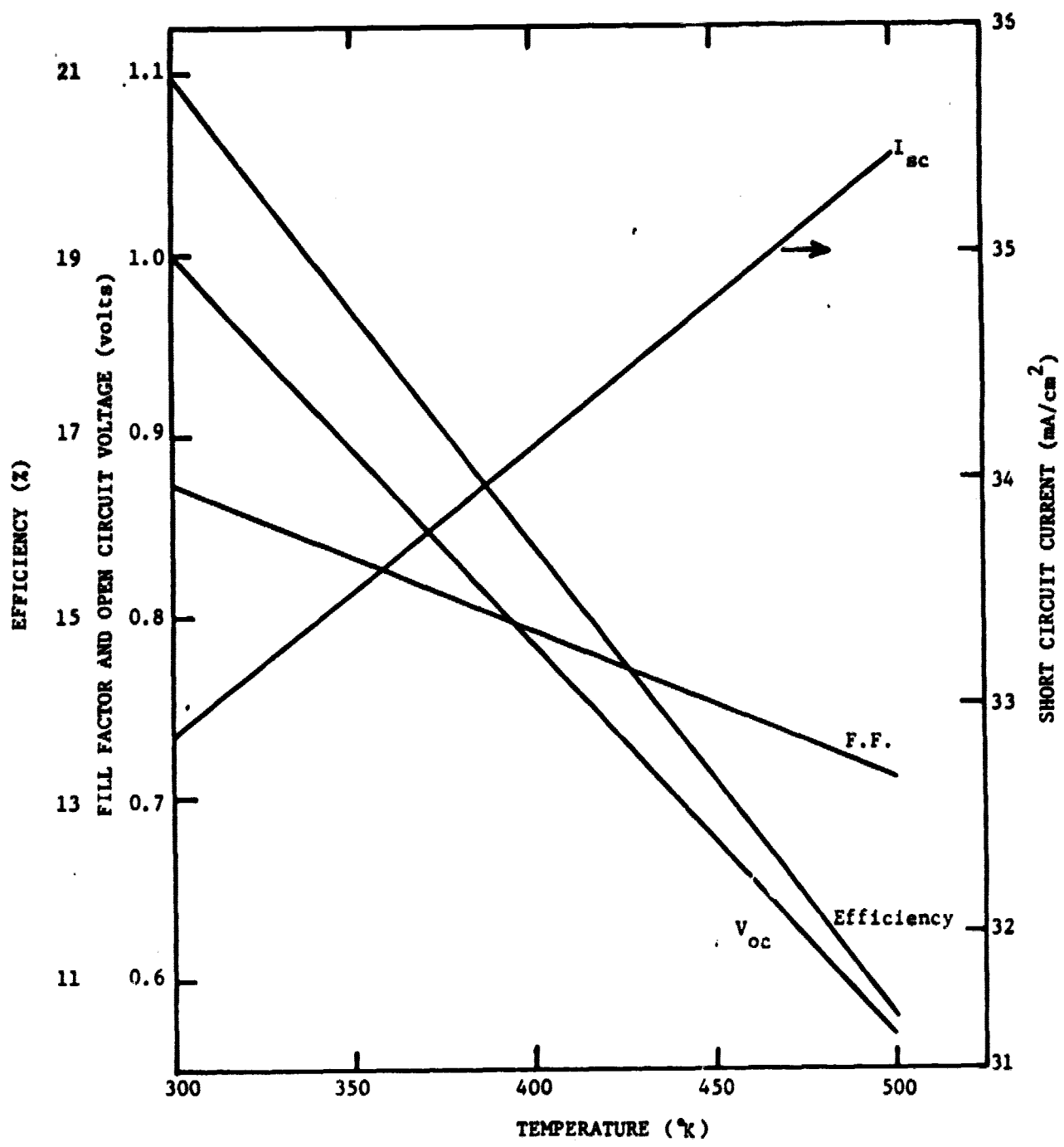


Figure 4. Dependence of Major Solar Cell Parameters on Temperature.

study are shown in Figure 5 for temperatures of 300°K and 500°K. As has previously been discussed [4], the peak efficiency at 300°K occurs almost exactly at the GaAs base layer composition. As the composition is varied from 0% AlAs to increasing percentages, the open circuit voltage increases but the short circuit current decreases. These opposite changes give rise to a rather flat peak in efficiency.

At 500°K the efficiency peak is seen to be shifted to higher AlAs percentages and consequently to higher bandgaps. The peak efficiency occurs at about 20-22% AlAs which corresponds to an energy bandgap of about 1.70-1.73 eV.

Higher temperature of operation thus causes a shift of the optimum bandgap to higher values. This is seen in Figure 6 for three different temperatures. At 400°K the AlAs composition is approximately half that for the optimum composition at 500°K. At 400°K the improvement in efficiency over that achieved with GaAs as the base layer material is about 0.3 percentage point which may be too small to justify the added complexity of an AlGaAs base layer cell. At 500°K the enhanced efficiency is about 1.3 percentage points above a GaAs cell and represents a significant increase.

#### 4. EFFECTS OF SOLAR INTENSITY ON PERFORMANCE

The optimum semiconductor bandgap or composition for the base layer is also a function of solar intensity at which the cell is to be operated. This is shown in Figure 7 where peak efficiency is shown as a function of composition at three different solar intensities and at 500°K. The 1 sun curve is the same as that in Figure 5 and shows a peak in the range of 20-22% AlAs. At 100 and 500 suns the peak efficiency occurs at a lower composition of around 15-16% AlAs.

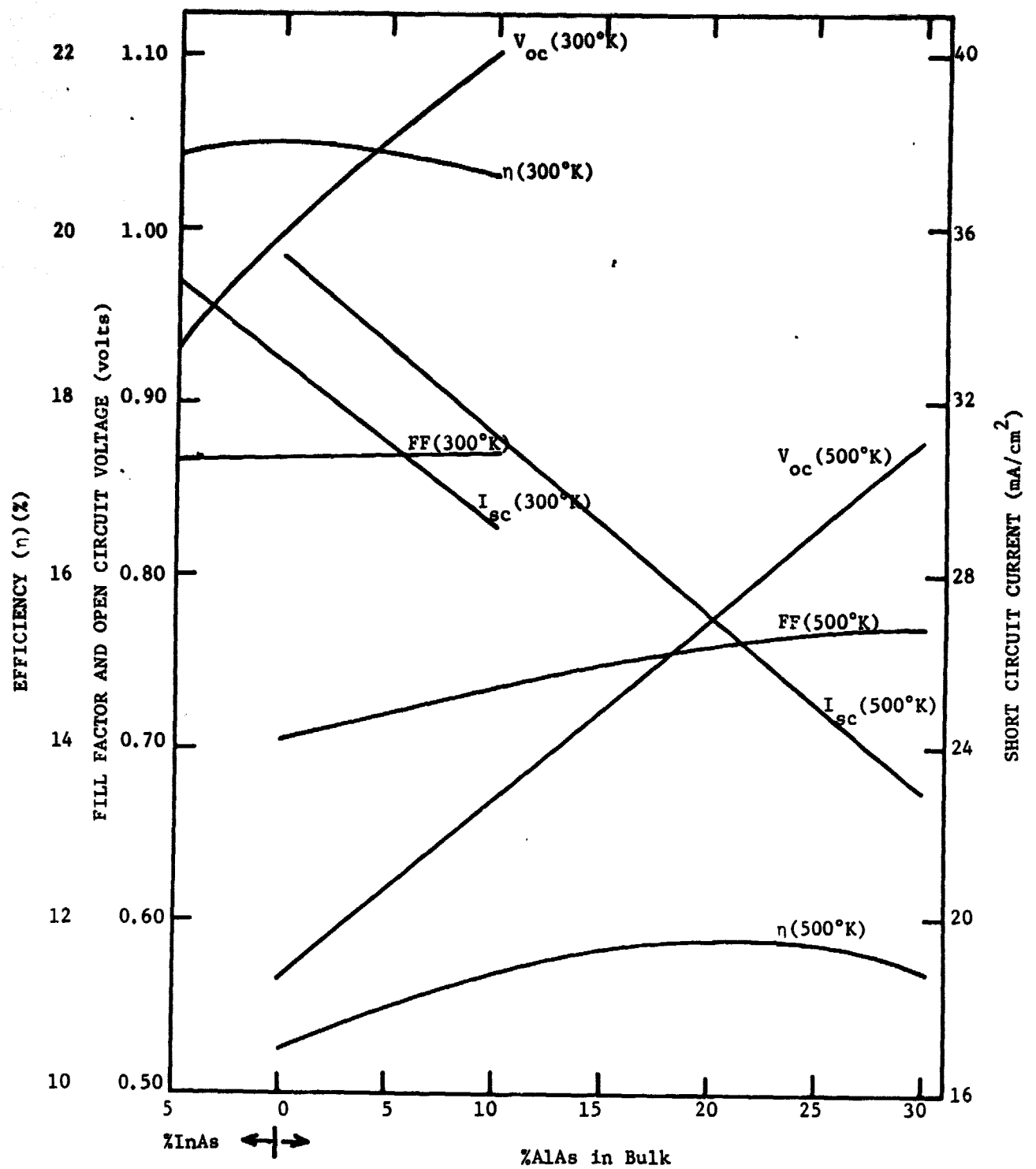


Figure 5. Solar Cell Parameters as a Function of Base Layer Composition.

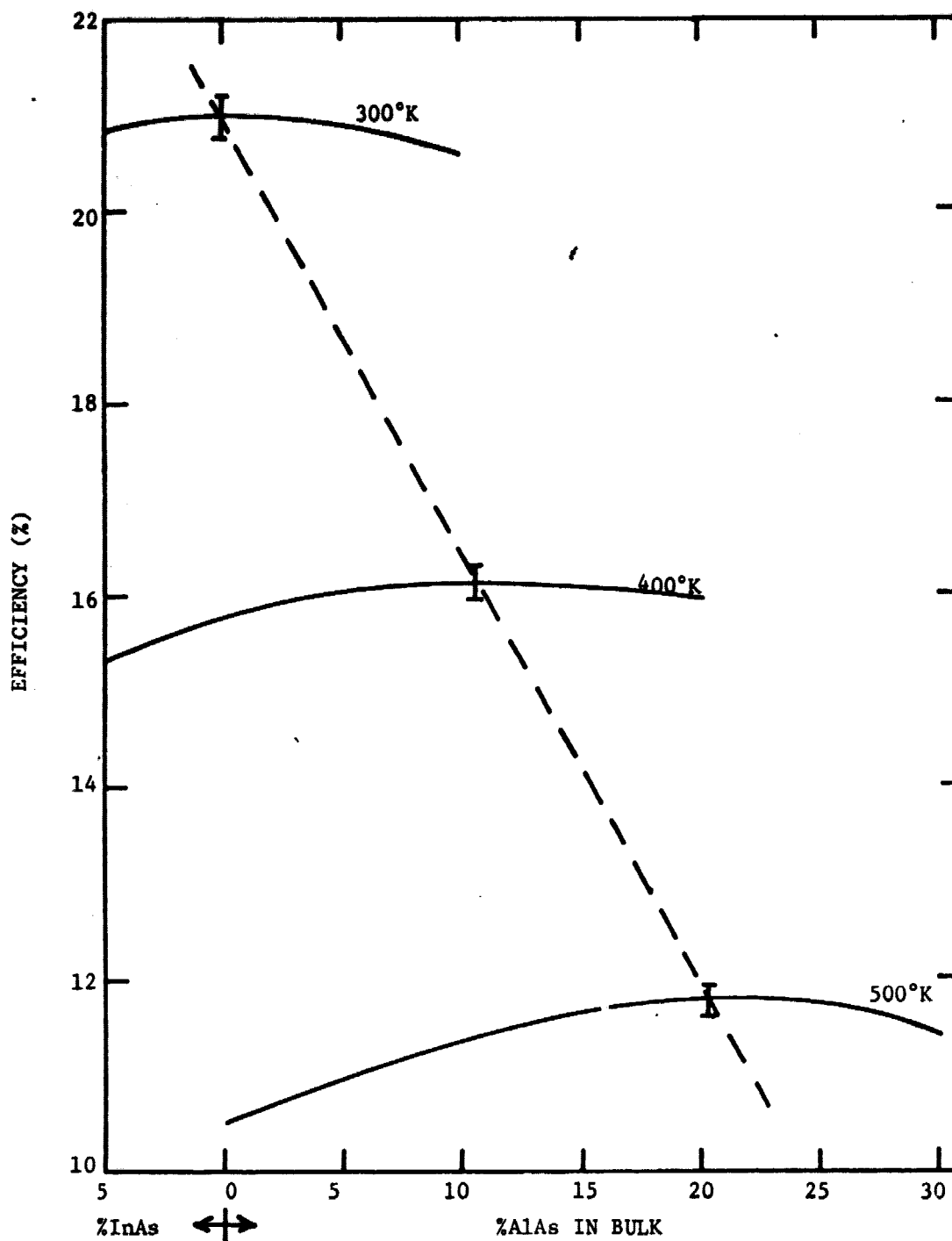


Figure 6. Peak Efficiency as a Function of Composition at Different Temperatures.



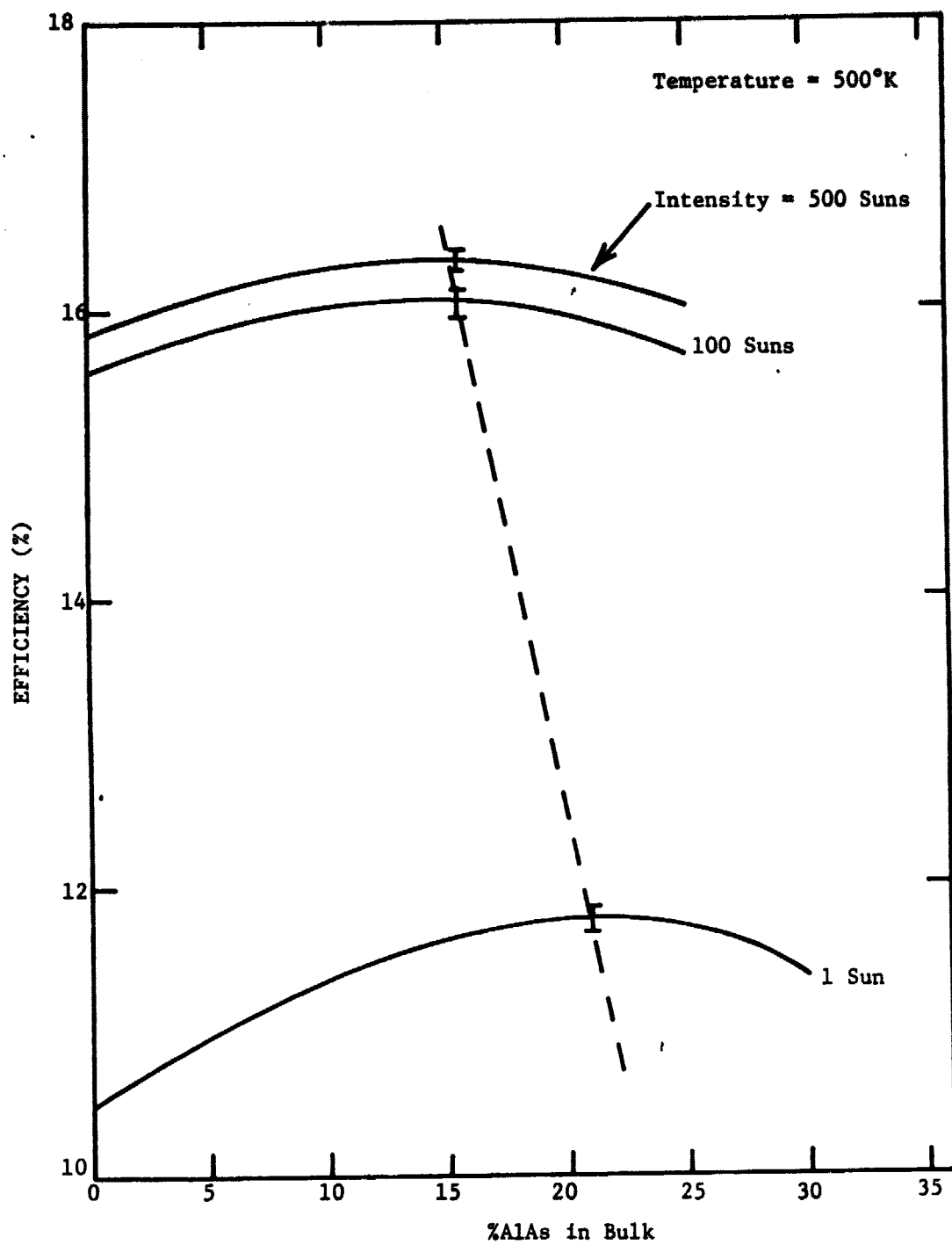


Figure 7. Peak Efficiency as a Function of Base Layer Composition for Different Solar Intensities.

A simple physical explanation of the decrease in optimum bandgap with increasing intensity is not easily obtained. From simple device models one expects the short circuit current to increase linearly with intensity at a fixed temperature and the voltage to increase logarithmically with increasing intensity. Both of these increases were found to be approximately valid from the exact computer analysis.

The fill factor is also expected to increase because of the increasing open circuit voltage. This expected variation of fill factor was not found, however, in the numerical calculations. The fill factor was in fact found to peak at a solar intensity of about 100 suns and then to decrease at higher solar intensities. This is shown in Figure 8 for two different base layer compositions of 0% and 25% AlAs. Also shown in Figure 8 are peak efficiency curves for the same compositions. The efficiency is seen to peak at about 300-500 suns and then decrease because of the rapid decrease in fill factor.

The decreasing fill factor can be traced to high injection effects occurring in the cell at high solar intensities and high temperature and its detrimental effect on efficiency. Referring back to Figure 2 it is seen that at 500°K, high injection effects with an  $m$  factor of about 2 begin to occur at a current density of about  $3 \text{ amp/cm}^2$  which is about two orders of magnitude above the  $J_{sc}$  line for 500°K. Thus at about 100 suns and 500°K the cell begins to operate under high injection conditions and this is responsible for the low fill factor above about 100 suns.

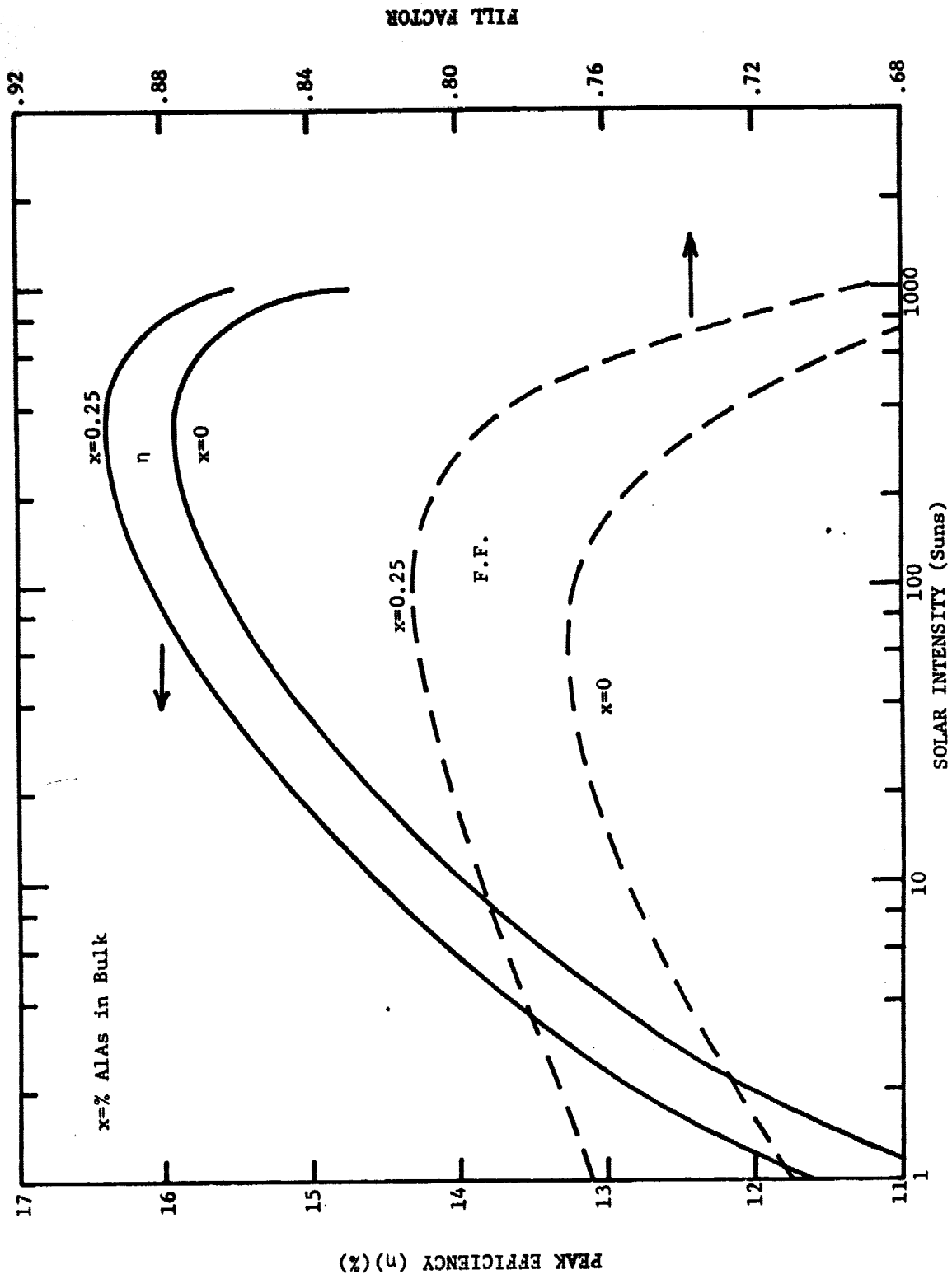


Figure 8. Changes in Peak Efficiency and Fill Factor as a Function of Solar Intensity.

## 5. SUMMARY AND CONCLUSIONS

In this work the effects of temperature and illumination intensity on the optimum base layer composition of AlGaAs solar cells has been investigated. A numerical computer program has been used to model in detail the properties of specific solar cell structures. The thicknesses of the various solar cell regions have been taken as fixed in this study and consequently the calculated efficiencies may not be the absolute maximum. However, the calculated results are expected to be close to the optimum values.

The optimum bandgap shifts to larger values and the optimum AlGaAs material shifts to larger AlAs percentages as the operating temperature increases. At 500°K 1 sun operation the optimum bandgap was found to be about 1.7 eV and to occur at 20-22% AlAs.

One of the most important results of this work is the finding that maximum efficiency peaks as a function of solar intensity. For 500°K operation the peak was found to occur at about 500 suns. This peak arises from the onset of high injection effects at high temperature and high intensities. In an actual cell other factors not considered such as surface layer sheet resistance can also give limiting efficiency effects. However, high injection is an intrinsic limiting effect which must be considered for high temperature, high intensity solar cells.

## REFERENCES

1. P. Rappaport, "The Photovoltaic Effect and Its Utilization", RCA Rev. 20, Sept. 1959, pp. 373-397.
2. M. B. Prince, "Silicon Solar Energy Converters", J. Appl. Phys. 26, May 1955, pp. 534-540.
3. J. J. Wysocki and P. Rappaport, "Effects of Temperature on Photovoltaic Solar Energy Conversion", J. Appl. Phys., 31, March 1960, pp. 571-578.
4. J. E. Sutherland and J. R. Hauser, "Optimum Bandgap of Several III-V Heterojunction Solar Cells", Solid State Elec. 22, January 1979, pp. 3-5.
5. J. E. Sutherland and J. R. Hauser, "Computer Analysis of Heterojunction and Graded Bandgap Solar Cells", Proc. Twelfth IEEE Photovoltaic Spec. Conf., Nov. 1976, pp. 939-944.
6. J. E. Sutherland and J. R. Hauser, "A Computer Analysis of Heterojunction and Graded Composition Solar Cells", IEEE Trans. on ED, ED-24, April 1977, pp. 363-372.
7. M. Neuberger, Handbook of Electronic Materials, vol. 2, III-V Semiconducting Compounds, IFI/Plenum Press, New York, New York, 1971.
8. A. Onton, M. R. Lorenz and J. M. Woodall, Bulletin of the American Physical Soc. 16, 1971, p. 371.
9. S. M. Sze, Physics of Semiconductor Devices, John Wiley, New York, New York, 1969.
10. M. R. Lorenz, R. Chicotka, G. D. Pettit and P. J. Dean, "The Fundamental Absorption Edge of AlAs and AlP", Solid State Comm. 8, 1970, p. 693.

## FIGURE CAPTIONS

- Figure 1. Heterojunction Solar Cell Device Structure.
- Figure 2. Dark I-V Characteristics for GaAs Base Layer Cell at Two Temperatures.
- Figure 3. Effects of Temperature on Light J-V Characteristics for GaAs Base Layer Cell.
- Figure 4. Dependence of Major Solar Cell Parameters on Temperature.
- Figure 5. Solar Cell Parameters as a Function of Base Layer Composition.
- Figure 6. Peak Efficiency as a Function of Composition at Different Temperatures.
- Figure 7. Peak Efficiency as a Function of Base Layer Composition for Different Solar Intensities.
- Figure 8. Changes in Peak Efficiency and Fill Factor as a Function of Solar Intensity.

## OPTIMIZATION OF AlGaAs SOLAR CELLS FOR RADIATION EFFECTS

J.P.C. Chiang and J.R. Hauser  
North Carolina State University  
Raleigh, NC 27650

### ABSTRACT

In this work some effects of radiation on the design of high efficiency AlGaAs solar cells are discussed. The optimum bandgap and composition of AlGaAs for maximum end-of-life efficiencies are discussed for concentration cells operating at high temperature. It is found that the optimum bandgap shifts to slightly larger values after radiation. An optimum p-n junction depth below the heterojunction of about 0.3  $\mu\text{m}$  is found both before radiation and after a radiation dose of  $10^{16}$  electrons/cm<sup>2</sup>.

## 1. INTRODUCTION

The AlGaAs/GaAs heterojunction solar cell has so far demonstrated the highest conversion efficiency of any single junction solar cell [1-3]. Previous studies have shown that such cells are very close to the optimum energy bandgap value for single junction cells [4,5]. AlGaAs/GaAs heterojunction cells also offer the potential for high concentration and/or high temperature operation. Concentration ratios as high as 500-1000 are presently being considered for such cells [6-9].

For operation in the space environment, the long term effects of electron (or other particle) irradiation are important design considerations. The average solar cell efficiency over some useful life expectancy is more important than the initial efficiency. In some space applications the end-of-life efficiency is the most meaningful efficiency value.

The high efficiency AlGaAs/GaAs solar cells are not presently used in space. However, they are being considered for a number of space applications. The solar space power station represents one potential large scale application of such cells. Because of the high cost of AlGaAs solar cells, they are most likely to be used in concentration systems with concentration factors on the order of several hundred.

Because of the large solar flux under concentration, high temperature operation of concentrator cells must also be considered. The temperature of a concentrator cell obviously depends on the method of cooling and the thermal resistance between the cell and any heat sink. The tradeoffs between the cost of heat removal equipment and loss of efficiency at



elevated temperatures are complicated system design factors. The approach taken in this work has been to explore optimum solar cell design at a high assumed operating temperature of 500°K. This may be too high for use in a practical solar cell application. However, the optimum solar cell design parameters found at 500 suns, 500°K operation are sufficiently similar to those found for 1 sun, 300°K operation that confidence can be gained in the fact that AlGaAs/GaAs heterojunction cells can be designed which will give near optimum performance over a wide range of concentration factors and temperatures.

## 2. SOLAR CELL MODELING

The solar cell model used in the present calculations is shown in Figure 1. The p-n junction is located slightly below an n-n heterojunction, with the wide bandgap window layer providing a low surface recombination boundary to the underlying narrower bandgap solar cell. The window layer was taken to be AlAs and with a thickness of 0.1  $\mu\text{m}$  in order to minimize optical absorption in this layer. The antireflecting layer was taken to be SiO with an optimum thickness of 700Å [10,11].

The material in which the p-n junction is located was taken as  $\text{Al}_{1-x}\text{Ga}_x\text{As}$  with the composition varied to select the optimum bandgap value for maximum efficiency. The thick base layer of the cell was taken to be p-type material. This was selected because of the much longer diffusion length for electrons than for holes.

The modeling of the material parameters as a function of composition and temperature has been discussed elsewhere [10,11]. For the effects of radiation on lifetime and diffusion length, the following equations were used:

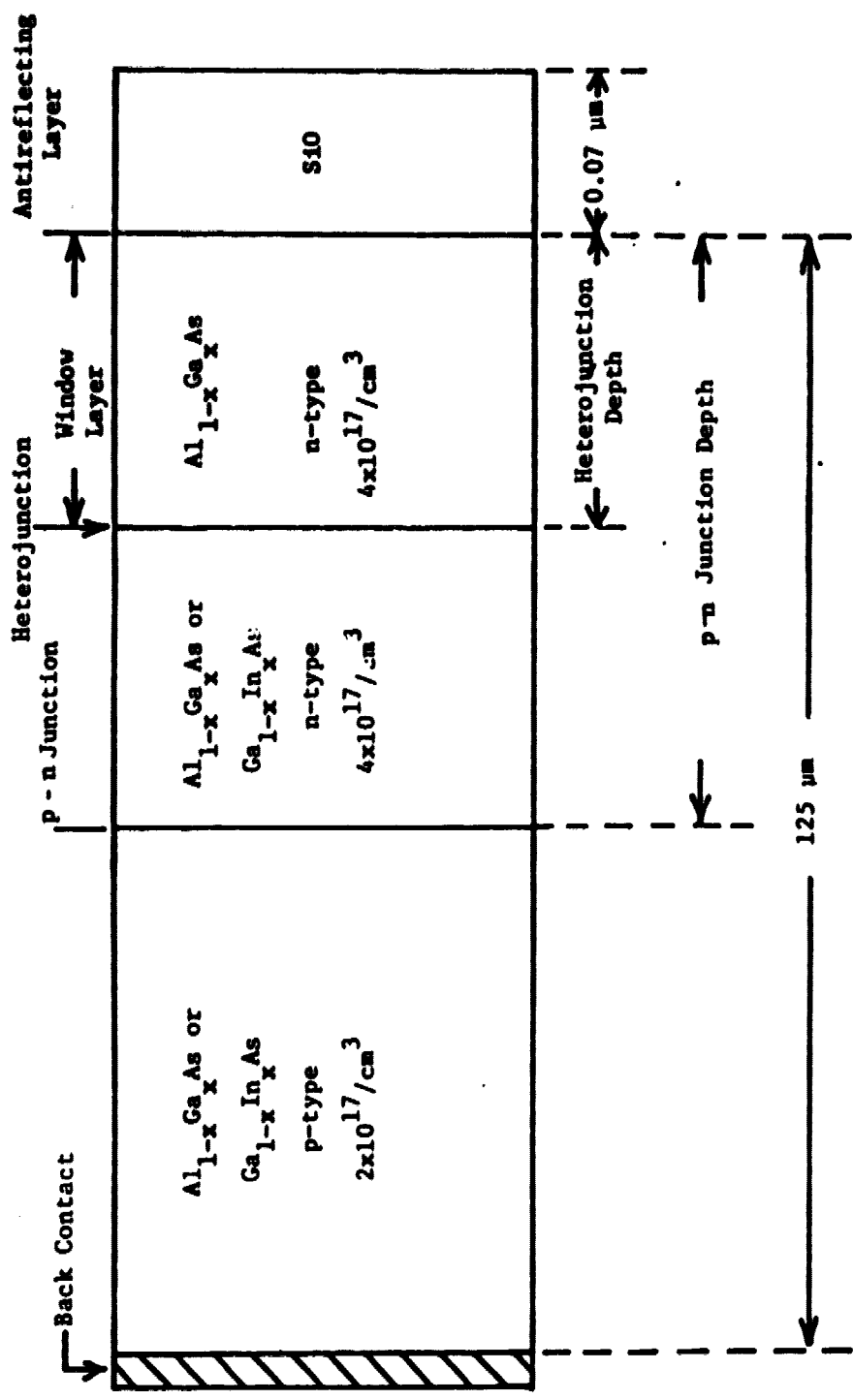


Figure 1. Heterojunction Solar Cell Device Structure.

$$\frac{1}{\tau} = \frac{1}{\tau_0} + K_{\tau} \phi, \quad (1)$$

$$\frac{1}{L^2} = \frac{1}{L_0^2} + K_L \phi, \quad (2)$$

where  $\tau_0$  and  $L_0$  are the unirradiated lifetime and diffusion length and  $\phi$  is the total electron radiation dose. The value of  $K_L = 7 \times 10^{-8}$  has been used in the calculations [12]. This value is the measured value for GaAs solar cells at room temperature. Since the optimum cell designs have AlGaAs compositions near that of GaAs, the use of the GaAs value should be reasonably accurate. A more serious limitation is the use of this value for cells operating at high temperatures (500°K for example). As opposed to Silicon, irradiation effects in GaAs are known to show annealing effects at fairly low temperatures. Thus at 500°K operation, the actual long term radiation damage coefficient is most likely less than that used in the calculations. The calculated results can thus be considered as worst case values for a given total radiation dose.

The analysis of the heterojunction solar cells was performed using a detailed numerical simulation of the semiconductor device equations. Details of this analysis have been presented elsewhere and will not be repeated here [10,11]. The calculations provide a detailed description of internal operating features as well as calculated terminal properties of short circuit current density, open circuit voltage, fill factor and peak efficiency.

### 3. CALCULATED RESULTS

In the first series of calculations, the performance degradation of a GaAs base layer cell was studied as a function of total electron radiation dose. The results are shown in Figure 2. The unirradiated cell, operating at 500 suns and 500°K has a peak efficiency value of slightly less than 16%. The efficiency remains relatively constant out to beyond  $10^{13}$  electrons/cm<sup>2</sup> and then falls to about 9% at  $10^{16}$  electrons/cm<sup>2</sup>. These results are similar to the 1 sun, 300°K results except for the magnitude of the efficiency which is slightly above 20% at low radiation doses.

The influence of base layer AlGaAs composition on solar cell parameters is shown in Figure 3. For the unirradiated case ( $\phi=0$ ) the results have been discussed in detail elsewhere [4,5]. The optimum composition is about 15% AlAs. Open circuit voltage increases with AlAs composition and short circuit current decreases as seen in the figure. For an electron dose of  $10^{16}$ /cm<sup>2</sup> the calculated results are similar except that the peak efficiency occurs at a composition of about 21% AlAs or at a slightly larger bandgap.

The effect of irradiation dose on the optimum semiconductor is shown in more detail in Figure 4 for several doses. The optimum bandgap shifts from about 1.6 eV (15% AlAs) at  $\phi=0$  to about 1.7 eV (21% AlAs) at  $\phi=10^{16}$ /cm<sup>2</sup>. The curves, however, are reasonably flat indicating that a cell designed with an AlAs composition anywhere within the range of 15%-21% has an efficiency value very near the maximum value over the total dose range studied.

The depth of the solar cell p-n junction below the heterojunction is an important design parameter for high end-of-life efficiency. To study

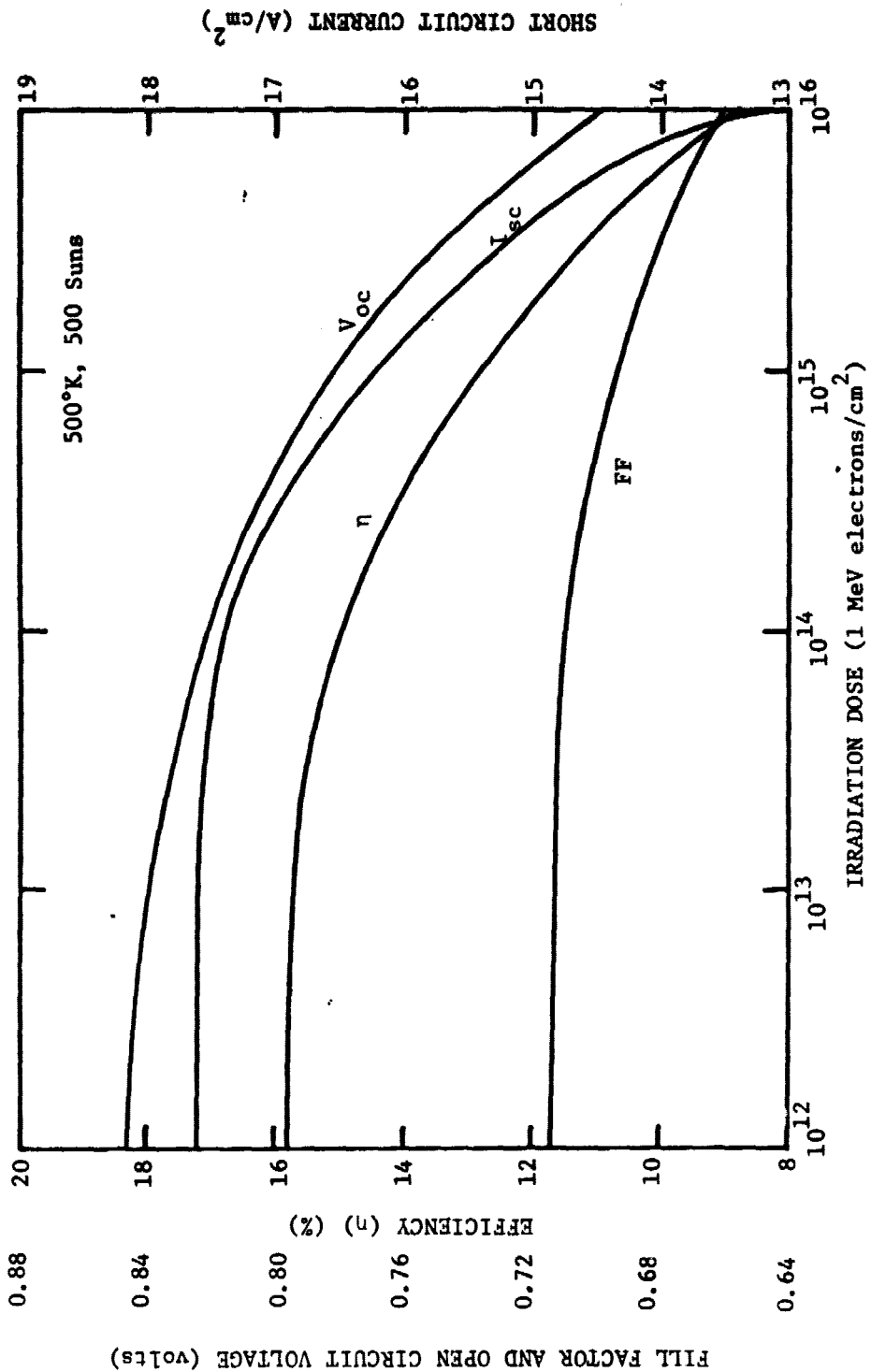


Figure 2. Effects of Electron Irradiation on Conventional GaAs Base Layer Cell Operated at 500 suns and 500°K.

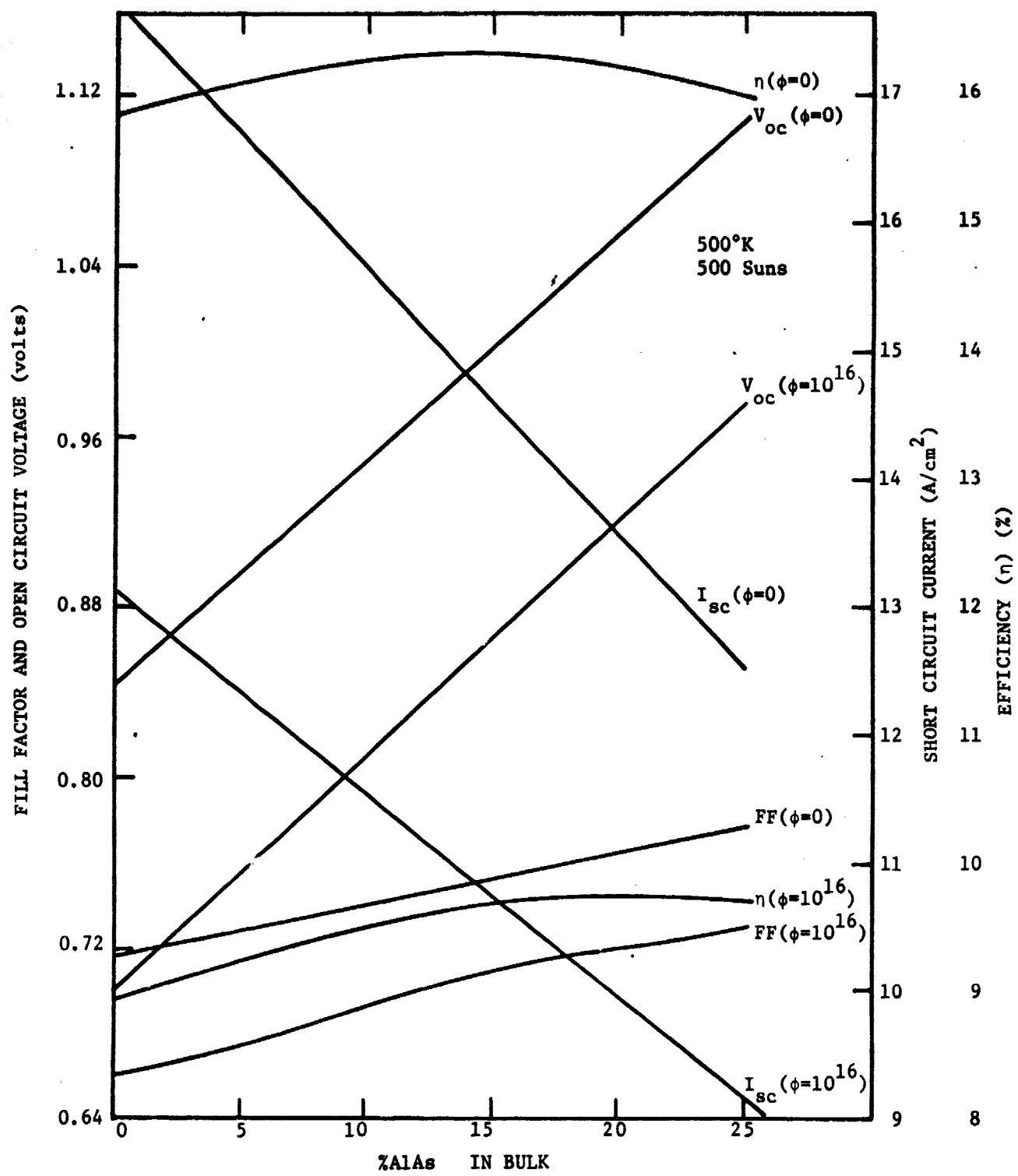


Figure 3. Solar Cell Parameters as a Function of Base Layer Composition.

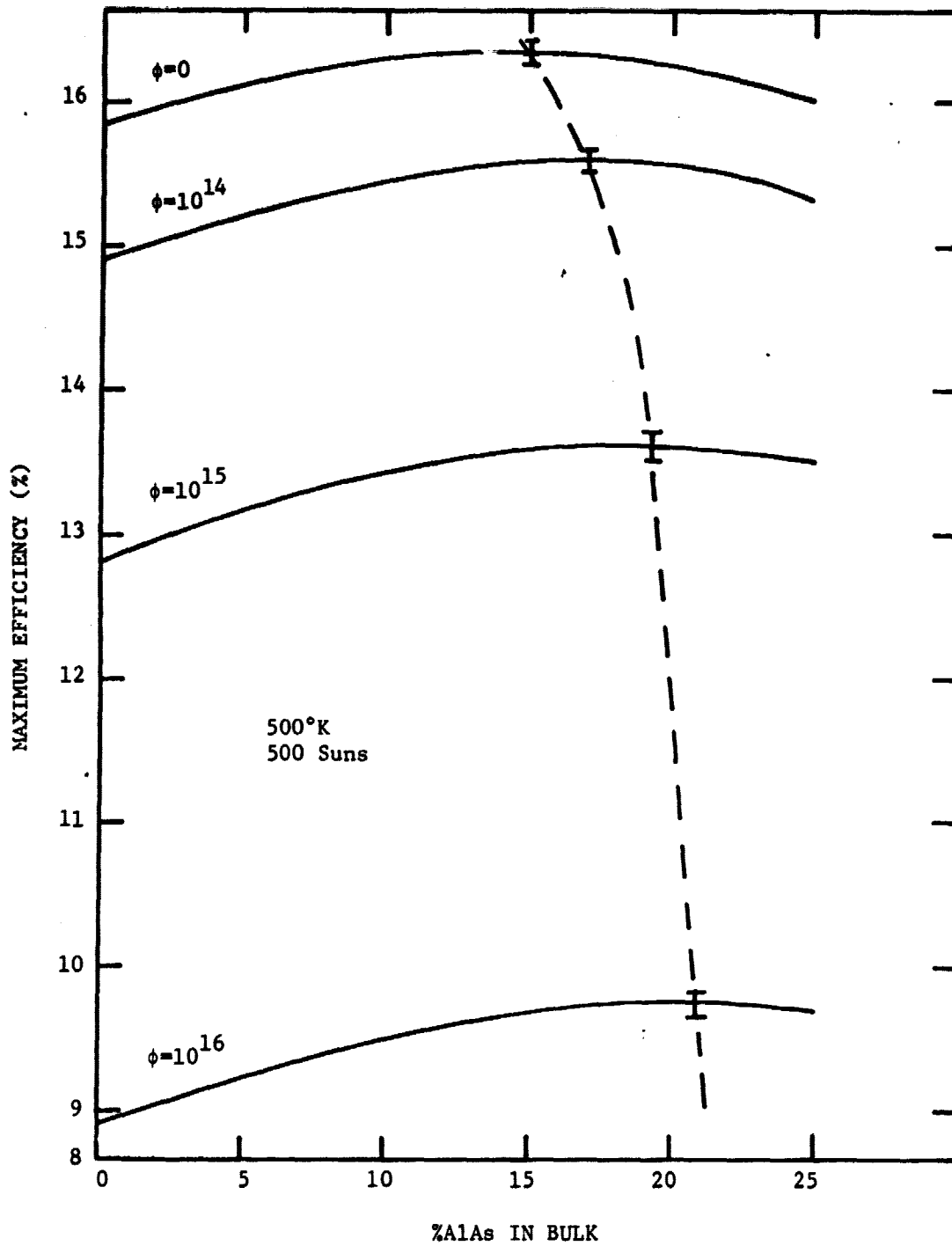


Figure 4. Effects of Electron Irradiation on Optimum Solar Cell Composition.

this effect at 500 suns, 500°K operation a series of calculations was made on cells with varying junction depths. The base layer semiconductor was selected as the value which gives maximum efficiency (15% AlAs) for the unirradiated cell. The short circuit current values obtained for a series of junction depths are shown in Figure 5. For the entire range of doses studied the 0.3  $\mu\text{m}$  junction depth gives the largest short circuit current. At  $10^{16}/\text{cm}^2$ , however, the 0.3  $\mu\text{m}$  curve is falling more rapidly than the  $x_j=0$  curve and the two curves should eventually cross with the  $x_j=0$  curve giving the largest current at very large doses.

A large junction depth ( $>0.6\mu\text{m}$ ) is seen to result in a rapid drop in short circuit current with irradiation. For a large junction depth a large percentage of the carriers recombine in the region between the heterojunction and the p-n junction when the diffusion length decreases due to the irradiation. The optimum junction depth decreases with irradiation dose as expected. However, the calculations show that over the range of irradiation doses out to about  $10^{16}$  electrons/ $\text{cm}^2$ , a junction depth of about 0.3  $\mu\text{m}$  is near the optimum value. This is illustrated in more detail in Figures 6 and 7 which show solar cell terminal parameters as a function of junction depth at unirradiated conditions (Figure 6) and at  $10^{16}$  electrons/ $\text{cm}^2$  (Figure 7). The solar cell parameters change much more rapidly with junction depth after irradiation than before irradiation. However, the optimum junction depth in both cases is around 0.2  $\mu\text{m}$  - 0.3  $\mu\text{m}$ .



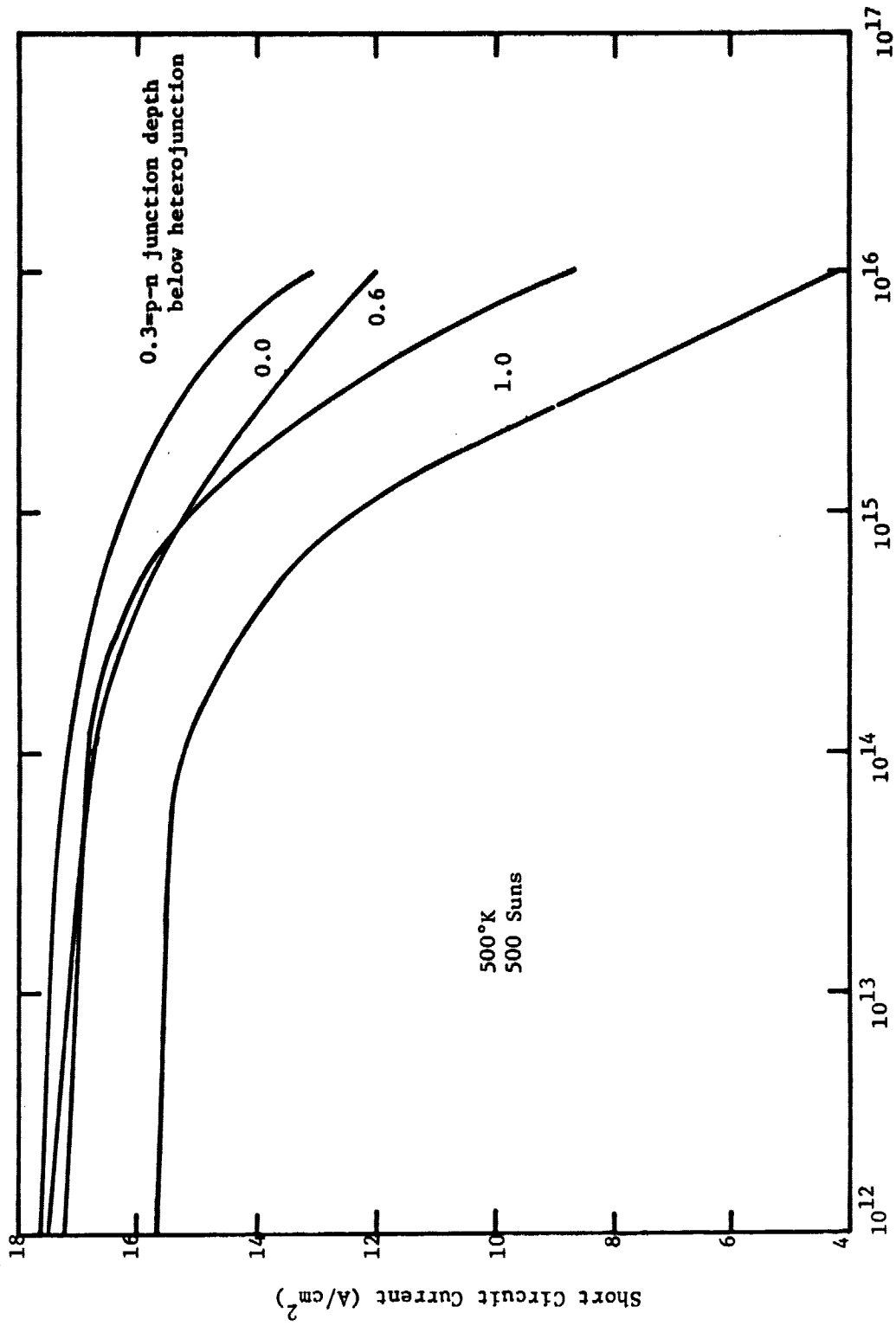


Figure 5. Short Circuit Current as a Function of Electron Dose for Various p-n Junction Depths. 10

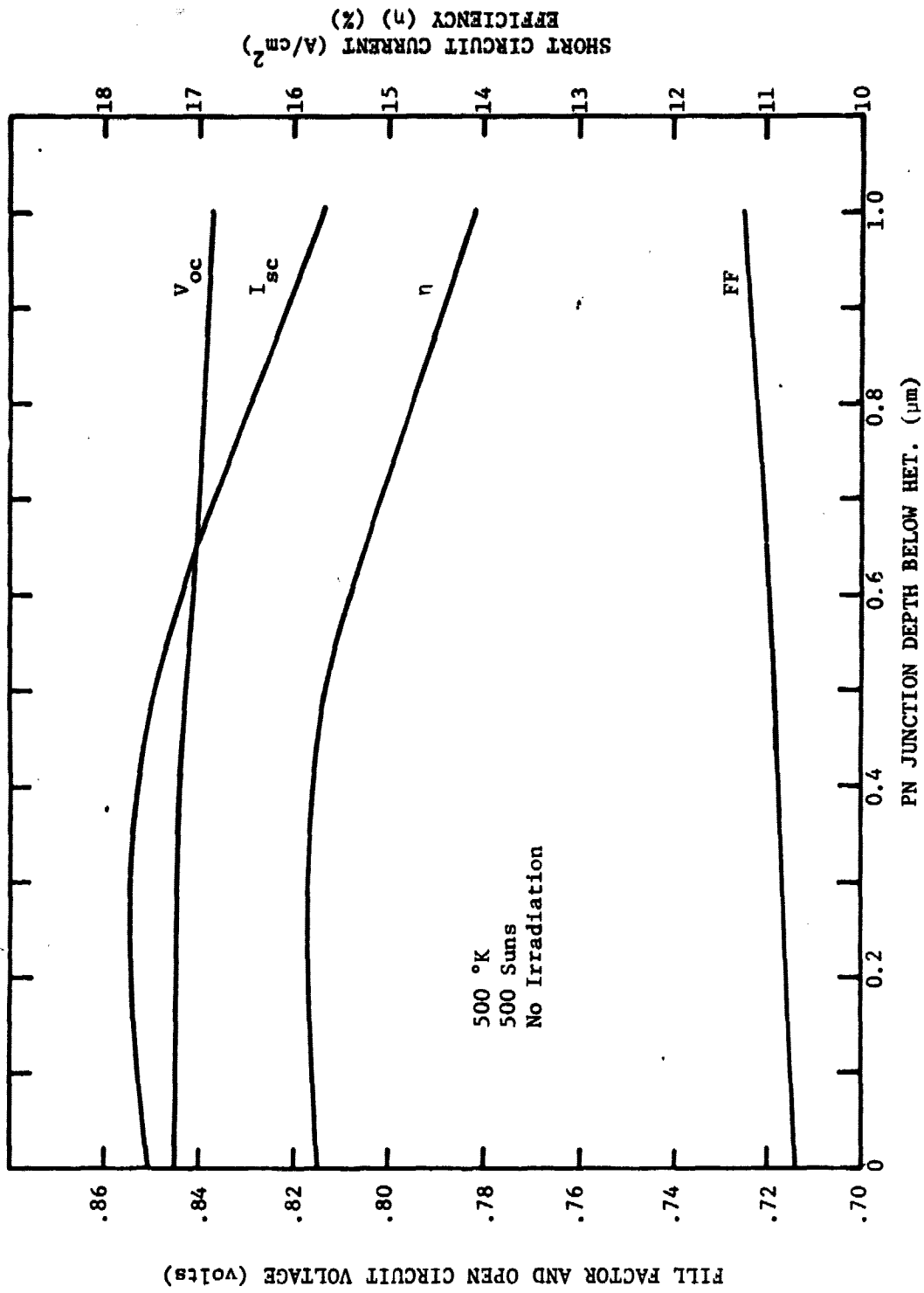


Figure 6. Solar Cell Parameters as a Function of Junction Depth for  $\phi=0$ . (500 suns, 500°K) 11

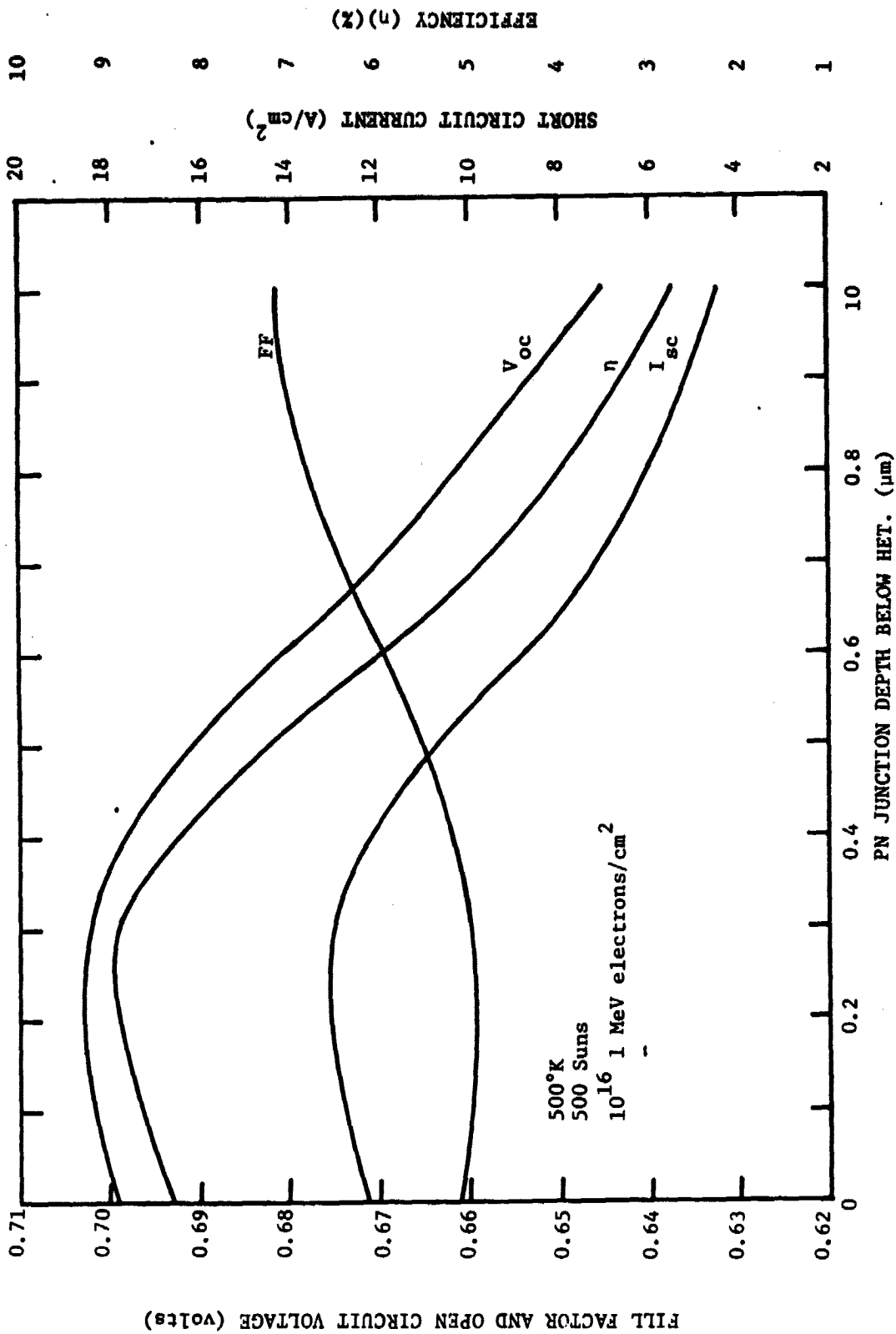


Figure 7. Solar Cell Parameters as a Function of Junction Depth for  $\phi=10^{16}$  electrons/cm<sup>2</sup> (500 suns, 500°K). 15

#### 4. SUMMARY AND CONCLUSIONS

In this work some effects of electron irradiation have been considered on the design of optimum AlGaAs solar cells. Irradiation has been found to increase slightly the semiconductor bandgap for highest efficiency. Also the optimum depth of the p-n junction below the heterojunction decreases slightly with electron irradiation. However, in both cases values of composition and junction depth can be found where operation is very near the maximum value achievable for irradiation doses up to  $10^{16}$  electrons/cm<sup>2</sup>.

These results indicate that AlGaAs solar cell designs should be capable of near optimum performance over a wide range of irradiation doses. While these results have been obtained for 500 suns and 500°K operation, similar conclusions are to be expected from these extreme operating conditions down to 1 sun, 300°K operation.

## REFERENCES

1. H. J. Hovel, Semiconductors and Semimetals, vol. 11: Solar Cells, Academic Press, NY, 1975.
2. H. J. Hovel and J. M. Woodall, "Theoretical and Experimental Evaluation of Ga<sub>1-x</sub>Al<sub>x</sub>As-GaAs Solar Cells", Proc. Tenth IEEE Photovoltaic Spec. Conf., November 1973, p. 25.
3. H. J. Hovel and J. M. Woodall, "Improved GaAs Solar Cells with Very Thin Junctions", Proc. Twelfth Photovoltaic Spec. Conf., November, 1976, pp. 945-947.
4. J. E. Sutherland and J. R. Hauser, "Optimum Bandgap of Several III-V Heterojunction Solar Cells", Solid-State Elec., 22, January 1979, pp. 3-5.
5. J. P. C. Chiang and J. R. Hauser, "Effects of Temperature and Intensity on the Optimum Bandgap of AlGaAs Solar Cells", to be published.
6. D. T. O'Donnell, S. P. Robb, T. T. Rule, R. W. Sanderson and C. E. Backus, "Performance of Silicon and Gallium Arsenide Concentrator Cells", Proc. Thirteenth Photovoltaic Spec. Conf., June 1978, pp. 804-809.
7. H. A. Vander Plas, L. W. James, R. L. Moon and N. J. Nelson, "Performance of AlGaAs/GaAs Terrestrial Concentrator Solar Cells", Proc. Thirteenth Photovoltaic Spec. Conf., June 1978, pp. 934-940.
8. J. Ewan, R. C. Knechtli, R. Loo and G. S. Kamath, "GaAs Solar Cells for High Solar Concentration Applications", Proc. Thirteenth Photovoltaic Spec. Conf., June 1978, pp. 941-945.
9. R. Sahai, D. D. Edwall and J. S. Harris, Jr., "High Efficiency AlGaAs/GaAs Concentrator Solar Cells", Proc. Thirteenth Photovoltaic Spec. Conf., June 1978, pp. 946-952.
10. J. E. Sutherland and J. R. Hauser, "Computer Analysis of Heterojunction and Graded Bandgap Solar Cells", Proc. Twelfth Photovoltaic Spec. Conf., November 1976, pp. 939-944.
11. J. E. Sutherland and J. R. Hauser, "A Computer Analysis of Heterojunctions and Graded Composition Solar Cells", IEEE Trans. on ED, ED-24, April 1977, pp. 363-372.
12. R. Loo, L. Goldhammer, B. Anspaugh, R. C. Knechtli and G. S. Kamath, "Electron and Proton Degradation in (AlGa)As-GaAs Solar Cells", Proc. Thirteenth Photovoltaic Spec. Conf., June 1978, pp. 562-570.

## FIGURE CAPTIONS

- Figure 1. Heterojunction Solar Cell Device Structure.
- Figure 2. Effects of Electron Irradiation on Conventional GaAs Base Layer Cell Operated at 500 suns and 500°K.
- Figure 3. Solar Cell Parameters as a Function of Base Layer Composition.
- Figure 4. Effects of Electron Irradiation on Optimum Solar Cell Composition.
- Figure 5. Short Circuit Current as a Function of Electron Dose for Various p-n Junction Depths.
- Figure 6. Solar Cell Parameters as a Function of Junction Depth for  $\phi=0$ . (500 suns, 500°K)
- Figure 7. Solar Cell Parameters as a Function of Junction Depth for  $\phi=10^{16}$  electrons/cm<sup>2</sup> (500 suns, 500°K).

COMPUTER ANALYSIS OF A DOUBLE HETEROJUNCTION  
SOLAR CELL STRUCTURE\*

J.P.C. Chiang and J.R. Hauser  
North Carolina State University  
Raleigh, NC 27650

The performance of a double heterojunction solar cell structure has been studied under 1 sun, AMO illumination. Such a structure has a reduced dark current over a conventional solar cell structure because of the minority carrier confinement between the two heterojunctions. The efficiency of such a cell, however, has been found to be lower than that of a conventional heterojunction solar cell because the loss of short circuit current more than offsets the increased open circuit voltage.

---

\*This work was supported by a NASA Langley research grant.

## 1. INTRODUCTION

A conventional AlGaAs/GaAs heterojunction solar cell consists of a thin, wide bandgap AlGaAs layer on top of a thick GaAs base layer. The p-n junction is typically located slightly below the heterojunction and within the GaAs base layer. The wide bandgap AlGaAs layer acts as a window layer to pass most of the photons but at the same time gives a low minority carrier interface recombination velocity at the surface of the GaAs layer. The AlGaAs/GaAs heterojunction solar cell has so far exhibited the highest conversion efficiency of any single junction solar cell [1-3]. Such cells have also been shown to be theoretically very near the optimum bandgap for single junction cells [4,5].

Further improvements in the efficiency of an AlGaAs/GaAs solar cell could be obtained if some means could be found to improve the short circuit current and/or the open circuit voltage. There are straightforward ways for achieving the maximum short circuit current. These include the use of multiple antireflecting layers or textured surfaces to reduce surface reflection and the achievement of long diffusion lengths to collect all of the optically generated carriers. The open circuit voltage is controlled by the short circuit current and the dark current of the cell. For large open circuit voltages a low dark current is necessary. Long diffusion lengths reduce the dark current as well as improve the short circuit current. In addition to the basic material parameters, device structures can be employed to influence dark current. In silicon solar cells the use of a back surface high-low p-p<sup>+</sup> junction has been used to reduce dark current and enhance open circuit voltage [6,7]. In III-V diodes a double heterojunction type of device structure has been used very successfully to reduce diode current in laser diodes [8-10].



In this work the application of the double heterojunction structure to solar cells has been explored. The motivation for this was the recognition as discussed above that such a structure can be used to reduce the dark current and hopefully increase the open circuit voltage of a III-V solar cell.

## 2. DOUBLE HETEROJUNCTION SOLAR CELL STRUCTURE

The basic solar cell structure studied is shown in Figure 1. An energy band diagram (for  $y=10 \mu\text{m}$ ) is shown in Figure 2. The structure is similar to a conventional AlGaA/GaAs heterojunction solar cell with the addition of a second heterojunction below the active cell at distance  $y$  from the semiconductor surface. In the figure the wide bandgap material is shown as pure AlAs. This has been used in the analysis to obtain the best possible performance. However the bandgap of  $\text{Al}_{1-x}\text{Ga}_x\text{As}$  does not change greatly for  $0 \leq x \leq 0.2$  so the results should also be representative of more practical compositions of 80%-90% AlAs.

Also the entire base layer is shown as composed of AlAs. In a practical double heterojunction cell the backside AlAs heterojunction would most likely be a thin layer grown on a GaAs substrate. This more practical structure would have another heterojunction present in Figure 1 between point  $y$  and the back contact, with the substrate being composed of GaAs. Such a structure was not considered here since it only complicates the analysis without introducing any additional important physical effects. Since the additional heterojunction would be away from the active solar cell region, it should not influence the results calculated here.

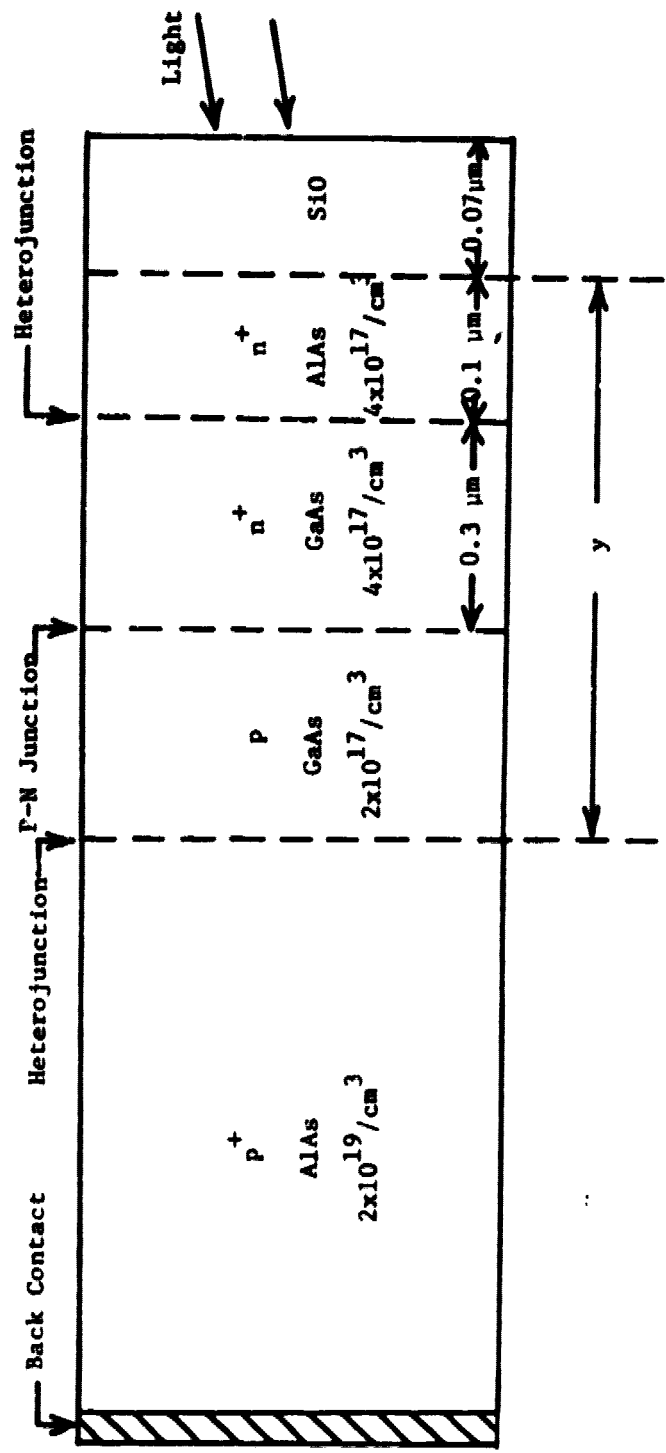


Figure 1. Double Heterojunction Solar Cell Structure.

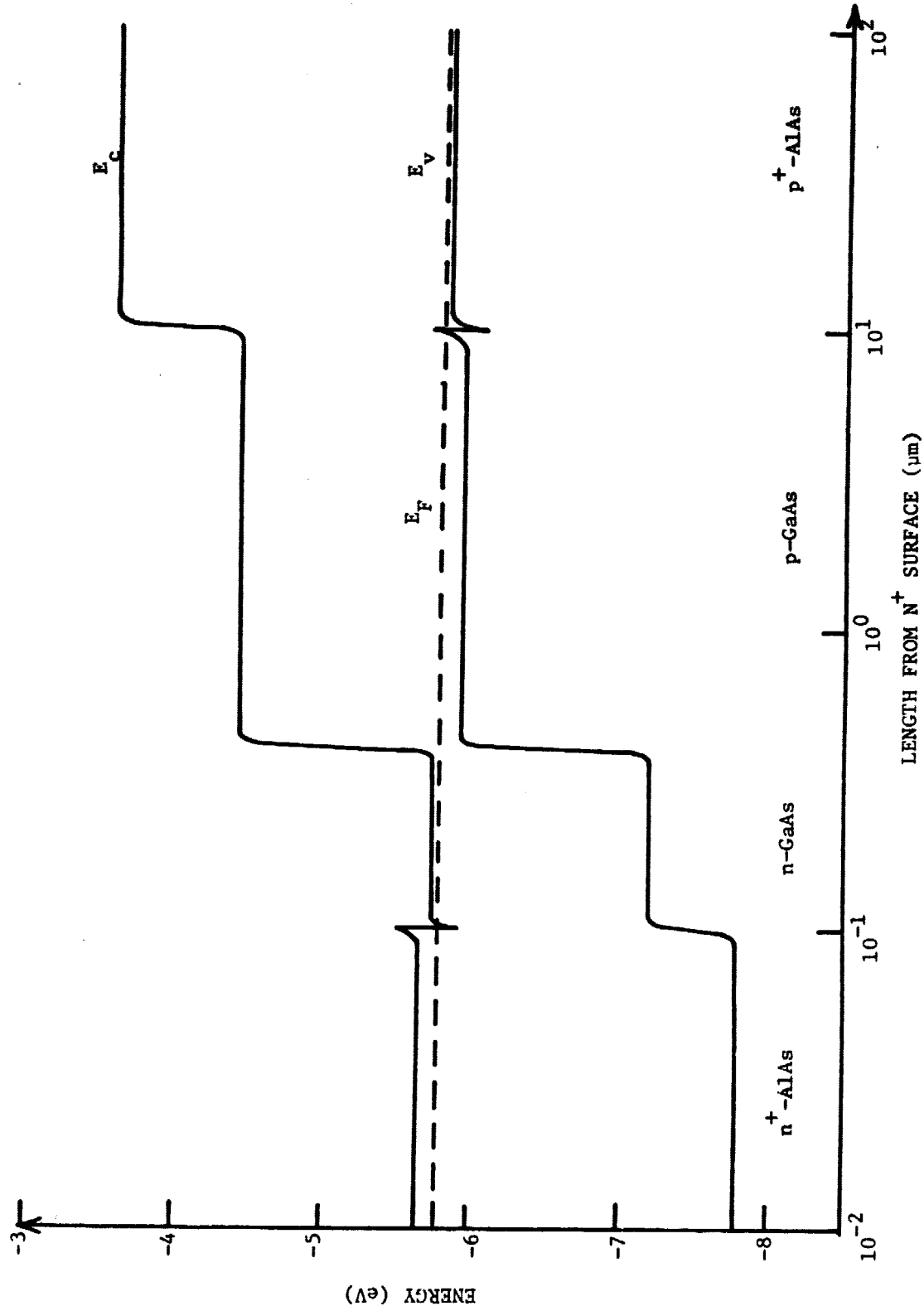


Figure 2. Energy Band Diagram for Double Heterojunction Solar Cell.

An antireflecting layer of 700Å has been taken as present on the surface. This is the optimum thickness for a conventional AlGaAs/GaAs solar cell [1,12]. The AlAs window layer thickness has been taken as 0.1 μm. As thin a layer as possible is desired for this layer. The p-n junction has been taken to be 0.3 μm below the heterojunction interface. This again is near the optimum junction depth for conventional cells. It may not of course be the optimum depth for a double heterojunction structure. However it was taken as fixed in the analysis in order to vary as few parameters as possible.

Finally an n<sup>+</sup>-p solar cell structure was selected for study. This differs in type from the p<sup>+</sup>-n structures which are typically produced experimentally for conventional AlGaAs/GaAs solar cells. A p-type base layer was selected because of the longer diffusion length for electrons than for holes. If the carrier confinement effect is to reduce the dark current of the cell, it should be more effective for a given value of  $\gamma$  with the p-type base layer than with an n-type base layer.

### 3. CALCULATED RESULTS

The solar cell structure shown in Figure 1 has been analyzed using a detailed numerical solar cell analysis program which is capable of handling a wide variety of heterojunction and/or graded bandgap structures. Details of the device modeling and numerical analysis techniques have been discussed elsewhere [11,12].

The value of diffusion length used in the calculations is one of the most critical parameters since the second heterojunction must be within about a diffusion length of the p-n junction in order for minority carrier

confinement effects to be important. The following empirical equations have been used to model the doping dependence of diffusion lengths:

$$L_n = \frac{8\mu\text{m}}{1 + (8 \times 10^{-19} / \text{cm}^3)N} \quad (1)$$

$$L_p = \frac{3\mu\text{m}}{L + (1.2 \times 10^{-18} / \text{cm}^3)N} \quad (2)$$

where  $N$  is the doping density. These equations give values of  $6.90 \mu\text{m}$  and  $2.03 \mu\text{m}$  for the GaAs n- and p-type regions of the active cell of Figure 1.

The results of the computer calculation with respect to dark current of the double heterojunction cell are shown in Figure 3 for different active cell thickness. The lower heterojunction must be located closer than about  $10 \mu\text{m}$  to have a significant effect on the dark current. The thickness must be reduced to only a few  $\mu\text{m}$ , however, to produce a large drop in dark current.

From first order device models, one can easily derive the relationship

$$J_o = J_\infty \tanh\left(\frac{W_p}{L_n}\right), \quad (3)$$

where  $J_\infty$  is the dark current for an infinitely thick p-type layer and  $J_o$  is the actual dark current for a given thickness  $W_p$ . This assumes an ideal minority carrier reflecting barrier at the heterojunction interface.

For the diffusion length from Equation (1) and a thickness of  $2.7 \mu\text{m}$  (overresponding to  $y=3 \mu\text{m}$ ), this simple model gives a dark current reduction of a factor of 2.68. At the largest voltage in Figure 3 the ratio of the two dark currents is 2.25 which is slightly less than the theoretical reduction. This difference is probably due to the presence of depletion region current which contributes some to the dark current.

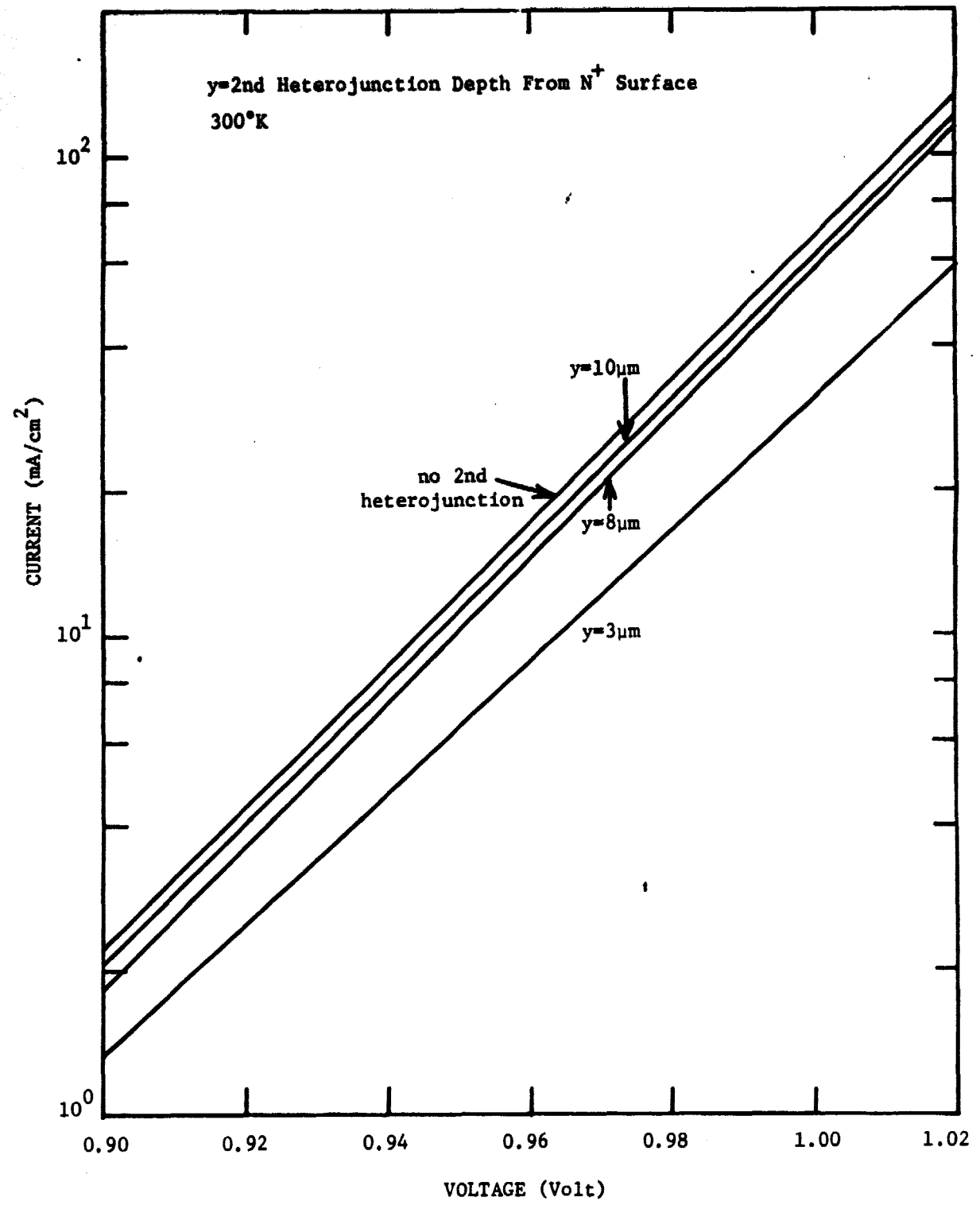


Figure 3. Dark Current for Double Heterojunction Solar Cell.

These calculations verify the expected dark current reduction for the double heterojunction cell. However this must be obtained at the expense of some short circuit current. Figure 4 shows the theoretical optical generation rate for the cell with an active layer thickness of 10  $\mu\text{m}$ . Beyond the second heterojunction ( $y=10 \mu\text{m}$ ) the generation rate drops to a very low value because of the wide bandgap. As the second heterojunction depth decreases, a larger part of the solar spectrum is lost due to incomplete optical absorption.

The important question concerning the double heterojunction solar cell is whether the improved dark current more than compensates for any loss in short circuit current. The results of Figure 5 clearly indicate that the answer is in the negative. This shows the complete light I-V characteristics of the double heterojunction cell for different cell thicknesses. Some minor improvement is seen in the open circuit voltage as expected. However, the loss in short circuit current more than offsets any increase in open circuit voltage. As the peak efficiency values show, the best efficiency occurs without the second heterojunction.

#### 4. SUMMARY AND CONCLUSIONS

These results demonstrate that a double heterojunction type of solar cell structure has a lower efficiency than a conventional type of heterojunction solar cell. While carrier confinement in such a cell does act to reduce dark current and increase open circuit voltage, the loss of short circuit current in such a cell more than offsets these advantages.

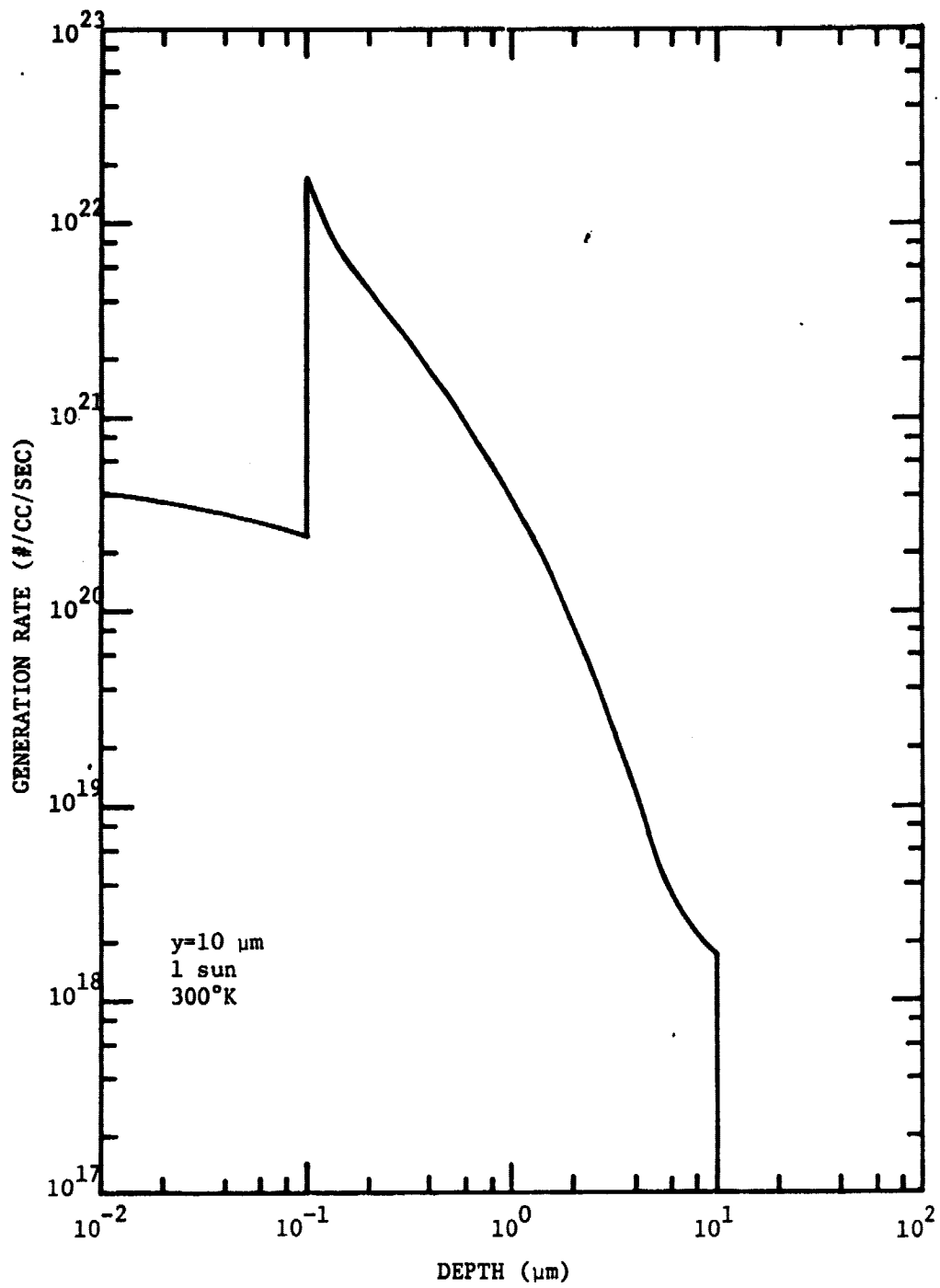


Figure 4. Optical Generation Rate for Double Heterojunction Solar Cell.



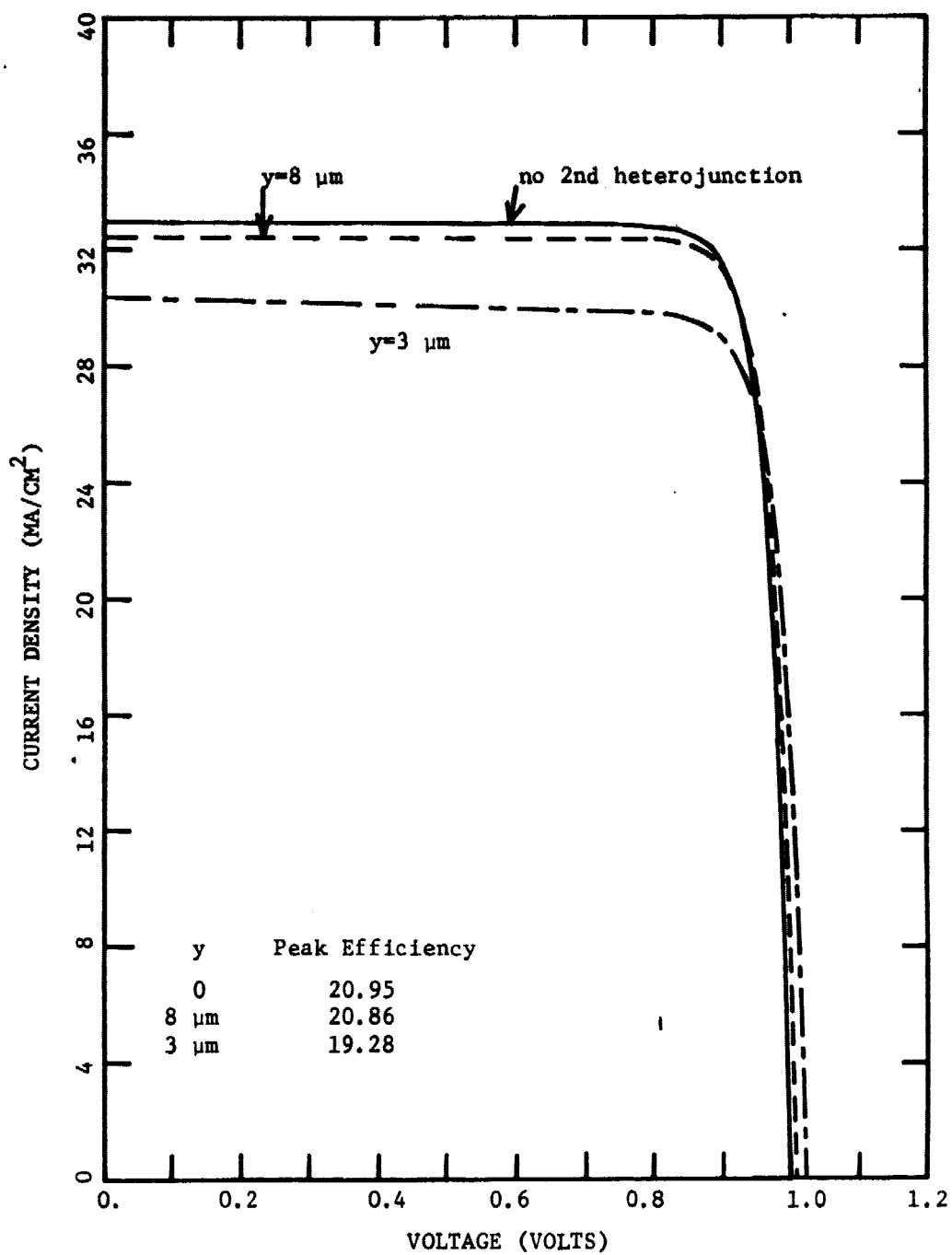


Figure 5. Light I-V Characteristics of Double Heterojunction Solar Cell.

These conclusions are somewhat dependent on the value of diffusion length which can be attained in the solar cell. If the diffusion length were 10 times as large as those used in the calculations, then some enhancement of performance would likely occur with the double heterojunction cells. However, such large diffusion lengths do not at present appear practical for GaAs material.

Even though the overall efficiency of the double heterojunction solar cell is less than that of a conventional cell, such structures might have some advantage as radiation resistant cells. They should degrade less rapidly with radiation than conventional cells because the diffusion length would need to be reduced below the active layer thickness in order to produce large degradations in performance. Also the active region of the double heterojunction cell is very thin. If such cells could be built without the need for a thick substrate such cells could potentially have a weight advantage for space applications.

## REFERENCES

1. H. J. Hovel, Semiconductors and Semimetals, vol. 11: Solar Cells, Academic Press, NY, 1975.
2. H. J. Hovel and J. M. Woodall, "Theoretical and Experimental Evaluation of Ga<sub>1-x</sub>Al<sub>x</sub>As-GaAs Solar Cells", Proc. Tenth IEEE Photovoltaic Spec. Conf., November 1973, p. 25.
3. H. J. Hovel and J. M. Woodall, "Improved GaAs Solar Cells with Very Thin Junctions", Proc. Twelfth Photovoltaic Spec. Conf., November, 1976, pp. 945-947.
4. J. E. Sutherland and J. R. Hauser, "Optimum Bandgap of Several III-V Heterojunction Solar Cells", Solid-State Elec., 22, January 1979, pp. 3-5.
5. J. P. C. Chiang and J. R. Hauser, "Effects of Temperature and Intensity on the Optimum Bandgap of Al<sub>x</sub>G<sub>1-x</sub>As Solar Cells", to be published.
6. J. Mandelkorn and J. H. Lamneck, "Advances in the Theory and Application of BSF Cells", Proc. Eleventh IEEE Photovoltaic Spec. Conf., June 1975, pp. 36-39.
7. M. P. Godlewski, C. P. Baraona and H. W. Brandhorst, Jr., "Low High Junction Theory Applied to Solar Cells", Proc. Tenth IEEE Photovoltaic Spec. Conf., November 1973, pp. 13-15.
8. I. Hayashi, M. B. Panish, P. W. Foy and S. Sumski, "Junction Lasers Which Operate Continuously at Room Temperature", Appl. Phys. Lett. 17, 1 August 1970, pp. 109-111.
9. Zh. I. Alferov, V. M. Andrew, D. Z. Garbuzov, Yu. V. Zhurlyayev, E. P. Morozov, E. L. Portnoi and V. G. Trofimir, "Investigation of the Influence of the AlAs-GaAs Heterostructure Parameters on the Laser Threshold Current and the Realization of Continuous Emission at Room Temperature", Sov. Phys. - Semicond. 4, March 1971, pp. 1573-1575.
10. J. C. Dymant, L. A. D'Asaro, J. C. North, B. I. Miller, and J. E. Ripper, "Proton-Bombardment Formation of Stripe-Geometry Heterostructure Lasers for 300K CW Operation", Proc. IEEE, 60, June 1972, pp. 726-728.
11. J. E. Sutherland and J. R. Hauser, "Computer Analysis of Heterojunction and Graded Bandgap Solar Cells", Proc. Twelfth Photovoltaic Spec. Conf., November 1976, pp. 939-944.
12. J. E. Sutherland and J. R. Hauser, "A Computer Analysis of Heterojunctions and Graded Composition Solar Cells", IEEE Trans. on ED, ED-24, April 1977, pp. 363-372.

## FIGURE CAPTIONS

- Figure 1. Double Heterojunction Solar Cell Structures.
- Figure 2. Energy Band Diagram for Double Heterojunction Solar Cell.
- Figure 3. Dark Current for Double Heterojunction Solar Cell.
- Figure 4. Optical Generation Rate for Double Heterojunction Solar Cell.
- Figure 5. Light I-V Characteristics of Double Heterojunction Solar Cell.

**END**

**DATE**

**FILMED**